PHYSICO-CHEMICAL CHARACTERIZATION OF RAW CLAYS USED IN POTTERY AT ILESI IN KAKAMEGA COUNTY - KENYA

By

STANSLAUS MANYENGO LUSAMBILI, BEd (Sc)

Reg. No. I56/24068/2012

A Thesis Submitted in Partial Fulfillment of the Requirements for the Award of the Degree of Master of Science (Chemistry) in the School of Pure and Applied Sciences of Kenyatta University

May, 2016

DECLARATION

I declare that this thesis is my original work and has not been presented for a degree or any other award in any other university/institution.

Signature …… Date ……
Stanslaus Manyengo Lusambili

We confirm that the work reported in this thesis was carried out by the candidate under our supervision and has been submitted with our approval as university supervisors.

Dr. Evans C. Ogwagwa
Department of chemistry
Kenyatta University
P.O Box 43844-00100 Nairobi

Signature…… Date ……

Dr. Alphonse W. Wanyonyi,
Department of chemistry
Kenyatta University
P.O Box 43844-00100 Nairobi

Signature……..Date ……

DEDICATION

To my father, the late Samuel Shikundi Lusambili and my mother Veronika Achekulwa Lusambili for sacrificing about all they laid their hands on for my education. I also dedicate this thesis my wife Victoria Sheila Lusambili, my daughters; Petronila Imbolokonye, Jacinta Kharikwa, Winnie Tsisika, Sharon Achayo, and my son Kelvin Ligushi for their patience during the period of this course. You all made a big sacrifice for me.

ACKNOWLEDGEMENT

My special thanks go to my supervisors Dr. Evans C. Ogwagwa and Dr. Alphonse W. Wafula for tirelessly directing and guiding me throughout the collection of data and writing of this thesis. I express my gratitude to all the teaching and non-teaching staff at Chemistry Department, Kenyatta University, for their assistance throughout this course.

I acknowledge the laboratory staff in the Chemistry and Civil Engineering departments of Jomo Kenyatta University of Agriculture and Technology, the directors of; Roads Transport and Infrastructure Research laboratory, ICRAF, KEBS and KALRO for allowing me to use their facilities for sampling and testing.

May I also sincerely thank Wycliffe Atinya Shisundi and Josephat Makomere Mukhaya of the Ilesi Traditional Pottery for supplying me with their mixtures of molded clays and facilitating the acquisition of the raw clays.

I thank the Government of Kenya through Teachers Service Commission for granting me three months study leave without which it would have been very difficult to collect data. Finally I thank the almighty God for granting me the opportunity to do this course.

TABLE OF CONTENTS

LIST OF TABLES

LIST OF FIGURES

ABBREVIATIONS AND ACRONYMS

ANOVA	Analysis of variance
ASTM	American Society for Testing and Materials
CEC	Cation exchange capacity
EDX	Energy dispersive X-ray spectroscopy
FTIR	Fourier Transform Infra-Red
ICRAF	International center for Research in Agroforesty
KALRO	Kenya Agriculture Livestock Research Organization
KEBS	Kenya bureau of standards
LOI	Loss on ignition
SEM	Scanning electron microscopy
SCBA	Sugarcane baggase ash
XRD	X-ray diffraction spectroscopy

ABSTRACT

Ilesi market in Kakamega County has been known for pottery for more than five decades in spite of the fact that the clays used have not been scientifically characterized. The potters register significant losses in their production due to swelling during molding, breakages during drying and firing. The objective of this study was to characterize the clays with a view to determining their suitability for pottery. Clay soils from Ilesi deposits in Kakamega County have been physically and chemically characterized and their suitability for pottery determined. Soil samples collected from the clay deposits under exploitation were pretreated by crushing, drying, milling and desegregation on standard sieves. The mineral composition of samples was determined by X-Ray Diffractometry (XRD) and Fourier Transform Infared spectroscopy (FTIR). The data showed presence of a dickite which is a kaolin (6.4-15.8%), albite (15.6-22.4%), and microcline (38.2-44.6%) which are fluxes and quartz (23.6-34.8%) which is filler. The elemental composition of the clays was determined as oxides using Energy Dispersive X-ray spectroscopy (EDX). The data showed the presence of alumina (19-22%), silica (63-67%), Fe_2O_3 (4.8-7.6%) and low percentage of CaO (0.23-1.49%). MgO and Na_2O were notably below detection limit. The suitability for pottery was determined by measuring the Atterberg limits and other physical properties. The soils showed plasticity index of (9.4-18.6%), porosity (14.16±0.09-31.18±0.83%), dry shrinkage (5.48±0.24-9.76±0.24%), fired shrinkage (5.24±0.24-13.10±0.24%), moisture content (25.03-42.35%) clay content (26-38%), green compressive strength (22.17±1.12-28.83±0.20 MPa) and fired compressive strength (24.92±0.37-49.23±1.35 MPa), among others. These data showed that the clays were suitable for pottery. Furthermore, five combinations (R2 to R6) were formulated by mixing the clays in various ratios considering the data of results above and using the Ilesi potters mixture, R1 as the control. Their physical properties were determined and R6 showed the best limits of physical parameters measured including losses on molding, drying and firing. The data has also shown that losses can be eliminated by proper handling and mixing of the clays.

CHAPTER ONE

INTRODUCTION

1.1 Background information

Ilesi traditional pottery was started at Ilesi market, which is situated 5 km from Kakamega town on the Kakamega- Kisumu road in 1963 (Amadala, 2013). The potters majorly fabricated water cooling pots for sale during market days at neighboring market centers. The activity has since grown into a cottage industry around Ilesi that makes approximately 20,000 pot products in a month, directly and indirectly employing approximately 1,000 people. Search in the literature reveals no information about characterization of the clays under use as much as they have been used for years. Furthermore, the users report losses due to breakages before and during firing of their products. This concern prompted a systematic study of the clays to determine their characteristics and hence the suitability for pottery.

Clay is a natural resource used in the manufacture of a number of products among them, fired bricks, refractory bricks, tiles, deep well drilling mud, biomedical implants, manufacture of paper and paints, tobacco pipes and pottery (Adelabu, 2012). Its usage for current and new applications will continue to grow since it is a cheap and environmentally friendly raw material. Most table wares like pots, urns, utensils, pestles, mortars are made from earthen clays. Applications and uses of clays in ceramics depend on their chemical and physical properties like plasticity, moisture content, porosity, particle size, shrinkage, firing temperature, strengths of structure, structure of clay, charge density, chemical substitution among others.

Pottery making involves molding and mixing raw materials, forming, drying and firing of the product. The potters at Ilesi follow these steps. They mix the black, brown, and grey clays in equal quantities. They add grog sand measuring half of the clay ratios by mass to the clay mixture. They use traditionally made kilns whose firing temperatures cannot be altered much (Gosselain, 1992) but have enabled them to remain in production. The potters however, still make some losses due to breakages in the process of forming and firing however losses due to kilning techniques are reduced by training and gaining experience in the art (Gossenlain, 1992). Pot making business can be improved by training and innovation which influences access to new markets.

The marketing is dominated by middle men who source pots especially for urban and tourist markets. The techniques that alter the visual and tactile characteristics of pottery correspond to the economic situation of the potters, their age and broad interaction networks through which their goods are consumed (Gosselain, 2000).

Clays for pot-making should have plasticity index of between 15-25% (Abuh, 2004; Allen, 1986; Wanyonyi, 2004), a porosity of 4-10% (Kirabira, 2003; Nweke, 2007), shrinkage of 4-17% (Allen, 1986; Kirabira, 2003), firing temperature of 700-1100°C (Bordeepong *et al*; 2012; Maggate *et al.*, 2010), fired strengths of 27 to 70 MPa (Allen, 1986; Parashar and Parashar, 2012). Measurement of these physical parameters can be used to determine suitability of clay for a particular use.

1.2 Problem statement and justification of study

Pottery in Kakamega County, is largely done through non-conventional methods. The clays have not been characterized and the recipe they use is not recorded but handed down orally and by practice from generation to generation making reproducibility impossible. The potters incur losses of between 20% and 30% due to swelling of clays during molding, cracking of pots during drying and breakages during firing. It is not clear whether these losses are due to the unsuitability of the clays or the handling of it during the production process. This study therefore, sought to characterize the Ilesi clays by determining their suitability in terms of requisite physical properties such as Atterberg limits, porosity, shrinkage limit, clay content, moisture content, clay body density, particle size, loss on ignition and pressure of rupture. It also sought to determine the most suitable method as well as mixing ratio for best results.

1.3 Hypothesis

The clays used for pot making in Kakamega County are suitable for pottery but are not handled appropriately.

1.4 General objective

To characterize and determine the suitability of the raw clays and recipe used by Ilesi traditional potters in Kakamega County for pottery.

1.5 Specific objectives

i). To determine the mineral content of Ilesi clays using X-Ray Diffraction Spectroscopy (XRD).

ii). To determine the elemental composition of the clays and grog sand using Energy Dispersive X-Ray Spectroscopy (EDX).

iii). To determine the physical properties (plasticity index, porosity, shrinkage limit, loss on ignition, compressive strengths, sieve analysis, density and moisture content) of the raw clays used, Ilesi mixture and formulated clay mixtures.

1.6 Significance of study

The study will document clay mineral quantities in the raw clays and their suitability for pottery making which will contribute to the clay literature in the county and county. The characterization will reveal what else the clays are suitable for and possibly spur diversification of products produced. The results may boost consumer confidence for importers and reduce poverty due to improved sales.

1.7 Scope

The study only covered the clays mined in Ilesi market clay deposits.

CHAPTER TWO

LITERATURE REVIEW

2.1 Introduction

Potters use raw clays for making ceramic pots. In most cases they do this without knowledge of the basic characteristics of clays for this purpose (Amponsah-Dacosta *et al*., 2013). This is not different to the potters at Ilesi who have used their raw clays for pottery over five decades.

2.2 Classification of clays

Clay is a natural, earthy and fine grained material comprised of a group of crystalline minerals known as clay minerals (Kirk and Othmer, 2004). They are generally plastic at appropriate water contents and will harden when dried or fired (Mukherjee, 2013). Flint clays and halloysites are however not plastic (Grim, 1962).

Clays are classified into Kaolins, Smectites, Mica, Serpentite, Vermiculite, Sepiolite and Pylophylite (Guggenheim and Martin, 1995). They are formed from hydrolysis and hydration of silicates, dissolution of limestone rocks, slaking and weathering of clay rich sedimentary rocks and as a product of hydrothermal decomposition of granite rocks (Lee, 1986). The feldspars in granite rocks decompose over very many years to yield kaolins, silica and potash or soda as shown by the equations (**1**) and (**2**) below.

$$2KAlSi_3O_{8(s)} + 3H_2O_{(l)} \rightarrow Al_2Si_2O_5(OH)_{4(s)} + 4SiO_{2(s)} + 2KOH_{(aq)} \qquad \text{Equation (1)}$$

$$2NaAlSi_3O_{8(s)} + 3H_2O_{(l)} \rightarrow Al_2Si_2O_5(OH)_{4(s)} + 4SiO_{2(s)} + 2NaOH_{(aq)} \qquad \text{Equation (2)}$$

When the KOH and NaOH formed dissolve due to effects of rain, the remaining clay minerals form kaolins that exist in four different structures, kaolinite, dickite, nacrite and halloysite, a hydrated analogue (Kirk and Orthmer, 2004). The other clay minerals like smectites, serpentines, illites and sepiolites are formed when some of the aluminium in the structure is replaced by magnesium, iron, calcium, or lithium (Bohn *et al.*, 2001). Kaolins are coarse, with a particle size of 2.0-3.0μm while smectites and micas have fine texture and particle sizes of below 0.5 μm (Heckroodt, 1991). Table 2.1 gives a list of some of the clays discussed below (Kirk and Orthmer, 2004).

Table 2.1: Examples of clay minerals

Clay	**Clay mineral**	**Formula**
Kaolins	Kaolinite	$Al_2O_3.2SiO_2.2H_2O$
	Dickite	$Al_4Si_4O_{10}(OH)_8$
	Nacrite	$Al_2O_3.2SiO_2.2H_2O$
	Halloysite	$Al_2O_3.2SiO_2.4H_2O$
Mica	Illites	$K_y(Al_4Fe_4.Mg_4Mg_6)(Si_{8-y})O_{20}(OH)_4$
Smectites	Montmorillonite	$Al_{1.67}Mg_{0.33}(Na_{0.33})Si_4O_{10}(OH)_2$
	Beidellite	$Al_{2.17}[Al_{0.33}(Na_{0.33})Si_{3.17}]O_{10}(OH)_2$
	Nontronite	$Al_{2.17}[Al_{0.33}(Na_{0.33})Si_{3.67}]O_{10}(OH)_2$
Fuller's earth	Palygorskite-Sepiolite	$(Mg, Al)Si_4O_{10}.4H_2O$

2.2.1 Kaolins

Kaolins are white to grey plastic clays formed by alteration of feldspar and muscovite. Whereas the primary kaolins result from residual weathering or hydrothermal alteration of silicates the secondary ones are formed by flow (Bohn *et al*., 2001). Kaolin polymorphs can only be distinguished by x-ray diffraction spectroscopy, XRD (Edward *et al*., 1976).

Kaolins have hexagonal crystals that form 1:1 layer structures. Because of the tightness of the structural bonds, kaolinite particles d-spacings of 0.72 nm are not easily broken

down which explains their low plasticity, shrinkage and swelling properties (Tan, 2011). The Kaolin sheets are held together by hydrogen bonds that prevent expansions which also prevents entry of polar molecules hence a very low cation exchange capacity (CEC) of 10 to 100mmolkg^{-1} (Bohn *et al*., 2001). Figure 2.1 shows the structure of a kaolinite (www.google.pubs.usgs.gov.).

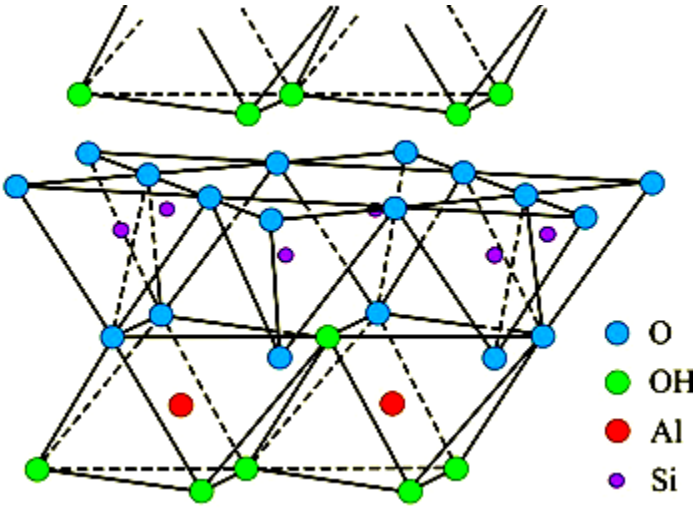

Figure 2.1: Diagramatic structure of kaolinite

Kaolins are the most widely used clays since they are pure and have high brightness, relatively low viscocity at high concentration (Sposito, 1989). They are used in pottery, manufacture of plastics, rubber, paint, cement among others.

2.2.2 Illites

Illite is a general term for clay constituents or argillaceous sediments that belong to hydrous mica group. It is a significant rock forming mineral being a main component of shales and other argillaceous rocks with a formula, $(K,H)Al_2(Si,Al)_4O_{10}(OH)_2.xH_2O$, where x represents the variable amount of water that exists in illites (Greenland and

Hayes, 1991). Figure 2.2 shows the structure of Illite with K^+ distributed within the inter layer (en.wikipedia.org).

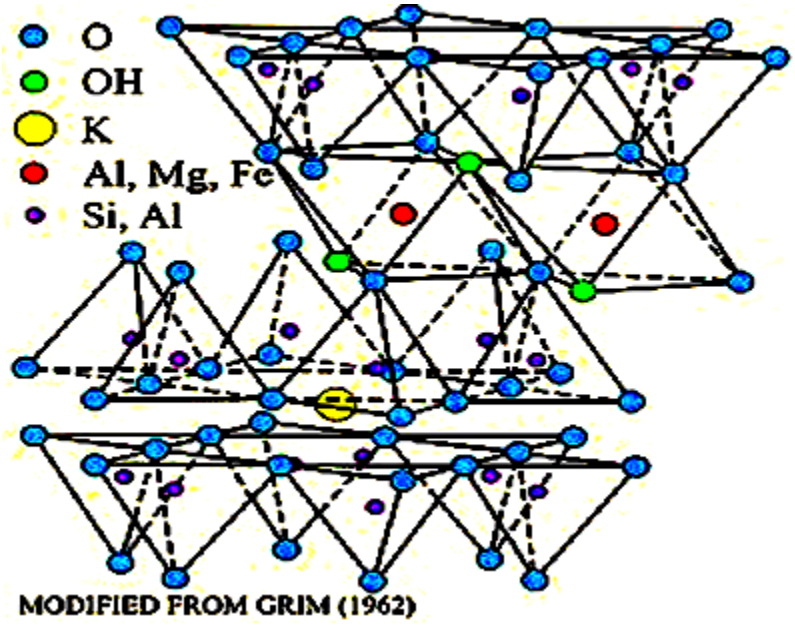

Figure 2.2: Diagramatic structure of illite

2.2.3 Smectites

Smectites are clay minerals that carry a lattice charge and usually expand when solvated with water or alcohol. Their 2.1 structures are arranged in silica-gibbsite- silica lattices. The aluminium in the $Al(OH)_3$ sheet is heavily substituted by iron and magnesium which gives the sheet a negative charge (Gieseking, 1975). Smectites have very small particle size with high affinity for water hence very plastic. They have low layer charge that causes a lot of isomorphic substitutions. The weak forces of attraction between crystal lattice enables polar molecules like water to enter the inter layer. This causes the clays to readily expand. The c-spacings are between 0.95 to 1.0 nm with high degree of interlayer solvation and exchangeable cation activity (Bohn *et al.*, 2001). They have a CEC of between 800 to 1200 $mmolkg^{-1}$ and highly pH dependent. Examples of smectites are

montmorillonite, beidellite and nontronite. They are usually used as metal ion adsorbents due to the negative charge. They are used in drilling muds, ceramics, foundry binders, sealants, iron ore pelletizer, adsorbents etc. Figure 2.3 shows the structure of montmorillonite indicating the position of magnesium and iron (II) on the octahedral sheet (http://pubs.usgs.gov/2001/01-041/index.htm).

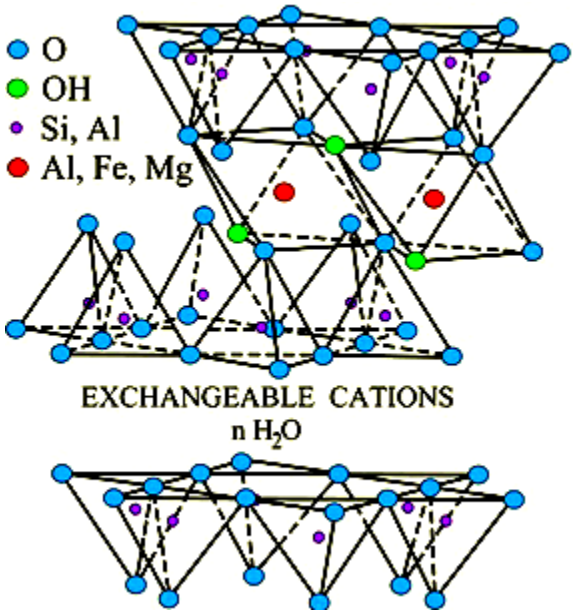

Figure 2.3: Structure of montmorillonite

2.2.4 Palygorskite-Sepiolite

Both palygorskite/attapulgite and sepiolite are hydrated magnesium, aluminium silicates of elongated chain structures. Sepiolite, however has higher magnesium content and large unit cell than palygorskite. These clays do not flocculate with electrolytes and are stable at higher temperatures, a property that determines their uses (Murray, 2002) like drilling fluids, paint manufacture, industrial floor absorbents, suspension fertilizers and medicinal suspension.

2.3 Composition of clays

The chemical substitution of aluminium by silicon, iron(III) and/or magnesium in clays generates positive and negative charges on the structure causing variations in the compositions of clays (Garrison, 1989). These compositions of clays vary in the minerals in which they occur. Clays exist in two structural sheets 1.1 that is gibbsite sheet $Al(OH)_3$ or $(Mg(OH)_2)$/ silicate sheet (SiO_2) as in kaolinite and the 2.1, which is a silicate sheet / gibbsite sheet /silicate sheet (Lee, 1986) as in smectite (Grimshaw, 1971; Kirk and Othmer, 2004). Table 2.2 shows compositions for some pure clay minerals (Grimshaw, 1971).

Table 2.2: Some clays with their percentage compositions

Clay	SiO_2	Al_2O_3	Fe_2O_3	TiO_2	CaO	MgO	Na_2O	K_2O
Kaolinite	45.44	38.52	0.30	0.16	0.08	0.08	0.66	0.14
Illite	51.22	25.91	4.59	0.53	0.16	2.84	0.17	6.09
Allophane	32.30	30.41	0.23	0.0	0.10	0.29	0.0	0.0
Montmorillonite	51.14	19.76	0.83	0.0	1.62	3.22	0.04	0.11

This data shows that clays have high percentage compositions of SiO_2, Al_2O_3 and low percentage composition of Fe_2O_3, CaO, Na_2O, TiO_2 and K_2O. Most clay deposits are found as mixtures of clay minerals or a clay mineral in presence of other minerals. Table 2.3 shows percentage compositions of raw clays in Saudi Arabia (Mohsen and El-maghraby, 2010).

Table 2.3: Mineralogy of local clays in a Saudi Arabia

Raw clay	Kaolinite	Illite	Quartz	Montmorillonite	Albite	Haematite
%White Clay	0	0	45	50	0	5
%Red Clay	40	0	18	12	16	14
%Green Clay	40	0	20	10	8	9

2.4 Naming of clays

Clays are complicated to name and therefore they are given names that are indicative such as:

i) pot clays for those that are used for pottery,

ii) china clay are usually plastic and give dense fired body,

iii) ball clays are plastic clays that burn into white material, they have very fine grain size and high plasticity,

iv) refractory clays are clays with high resistance to heat without loss of shape and

v) flint clays are virtually non plastic ones (Allen, 1986; Glenn and Burkett, 2002).

2.5 Pottery making process

Pottery making is usually carried out in six stages, acquisition of raw materials, clay processing, pot shaping, pot decoration, firing and post pot treatments like painting, application of water proofing resins (Kent, 2008). The number of steps taken by potters depends on their underlining cultures and market forces. Potters mix raw materials in ratios such as to improve the quality of their products and workability of the clay body. For example potters at Ilesi use equal ratios of the black, brown, grey clays and half grog sand while those at lower Thukela in KwaZulu-Natal prefer ratios of 60:40 and 50:50 black to red respectively (Kent, 2008).

Ceramic materials include clays, fluxes like alkali feldspars, talc, $3MgO.4SiO_2.H_2O$ or nephelinesyenite, $K_2O.3Na_2O.4Al_2O_3.9SiO_2$ and fillers like silica, SiO_2, beach sand or

grog, a coarse alumina, silica ceramic material. The filler reduces shrinkage and aids even drying.

Ceramics are made into paste and shaped at normal temperatures (Grimshaw, 1971). Firing gives them strength either by sintering crystallites together or partly melting them into a paste**.** The firing temperature range from 100°C to 1775°C causes changes in minerals or crystal phase through thermal expansion or shrinkage (Heimann and Franklin, 1979). The firing temperature also affects the color of the pot. A red colour shows an oxidizing atmosphere while black or grey indicates either insufficient firing time or reducing atmosphere (Tite, 2008). Firing at higher temperatures more than 1100°C vitrifies the clay by glazing the material increasing mechanical strength in addition to aesthetic effects.

Potters process clay to improve plasticity, workability and thermal shock resistance (Bronitsky and Hammer, 1986; Skibo *et al*., 1989). By mixing different types of clays in different proportions and combinations, potters are able to make many products (Rusovich-Yugai and Neklyudova, 2007). Some researchers have mixed their clays with waste materials like ground glass or sugarcane baggase ash, SCBA as fillers (Tonnayopas, 2013) and formed pots.

2.6 Important characteristics of clays

Some of the physical characteristics that determine use of clays for pottery are plasticity, compressive strength, porosity, shrinkage, firing temperature and particle size. There are

three major ways of characterizing clays in order to determine their uses, namely physical characterization, use of organic stain reactions and use of analytical instruments.

2.6.1 Physical characterization

In this characterization, the physical parameters listed below are determined and then compared with data in literature.

2.6.1.1 Plasticity Index

Plasticity is the property of clay such that when mixed with sufficient amount of water undergoes deformation by application of slight pressure and retention of the deformed shape after release of the pressure (Ghildyal and Tripathi, 1986). Some researchers have used values of plasticity index to characterize clays (Amponsah *et al.*, 2013). In this characterization the plastic and liquid limits are determined which indicate the range of workability of clay body. A plot of plastic limit on x-axis against plasticity index can be used to identify clay minerals (Bain, 1971). Clays with large particle size like kaolins have lower plasticity. Their structures have smaller water absorption capacity. Plastic and liquid limits are measured as percentage water that makes a soil plastic or liquid respectively. The plasticity index is determined as a ratio of the liquid and plastic limits. A plasticity index of 15 to 25% is considered suitable for pottery making.

2.6.1.2 Shrinkage

Shrinkage is the contraction of a clay body on drying or firing. Shrinkage depends largely on packing of particles in the clay body. The smaller the grain size the better the packing. Grain size can be reduced by grinding which arises close packing that reduces the

shrinkage effects. Linear shrinkage is measured as percentage contraction in millimeters. It is important because it determines the dimensions of a wet pot. Large and rapid shrinkage during drying and firing is one of the causes of pot breakages (Allen, 1986).

2.6.1.3 Porosity

Porosity is a measure of empty space in a soil material as a fraction to the total volume. It describes the fraction of voids or pores in a material. These are the empty spaces in a material where water can reside in a soil.

Porosity of a soil generally increases with increase in particle size. Kaolins have large porosity due to their large particle size hence low plasticity. They are preferred for pottery but for very plastic clays like most smectites, tempers are added to enable them allow water to dry out without cracking. Kaolinite occurs largely as discrete particles mainly in form of pseudo-hexagonal sub-idiomorphic platy crystals loosely attached to the walls of pores (Morris and Shepperd, 1992). This cornflake arrangement produces extensive micro pore space. Entrapment of water results into static permeability reduction and is caused by clay expansion both within the structure and by increased separations of individual particles, this results into restriction and blocking of pore throats.

Porosity measurements give a very useful indication of the degree of vitrification and directly indicative of the volume shrinkage (Allen, 1986). For earthenware porosity increases up to 1000°C, though there is marked decrease in internal surface area as some

of the smaller particles dissolve. Beyond this, vitrification proceeds and porosity decreases to theoretical zero at 1220°C.

Porosity is determined by measuring the amount of water a fired clay body absorbs over a period of time. This parameter depends on duration of the soaking of the pot into water and hence its standards vary from country to country.

2.6.1.4 Compressive strength of clays

Strength of a clay body is associated with the effects of the hydroxyl of water either through cohesion forces or reactions with elements in the structures. Compressive strengths or modulus of rupture represent the amount of load a body can hold without breaking (Parashar and Parashar, 2012). It depends on the forces of attraction between the sheets and layers in the clay minerals. It is influenced by the water and accessory ions in the interlayer, c-spacings and type of clay mineral lattice (Ding *et al.*, 2001). Fired strength increases with firing temperature due to increase in crystal forms that increase the surface tension forces (Agbalajobi and Omoijuanfa, 2012). It is measured as a crushing force per unit area in MPa (Mbereyaho and Twubahimana, 2013).

2.6.1.5 Density

The density of a clay body is the ratio of its mass to its volume. The densities of clay bodies increase with increase in temperatures of the clay bodies. The glass formation continues to increase the density until its maxima though this maxima is practically close to the minima of porosity for the same clay body.

Glass undergoes a glass transition within a range of temperatures in which physical properties like density, viscosity, heat capacity, porosity are changed reversibly by appropriate heat treatment (Thompson, 1995).

As the clay crystal phase changes between 1000°C to 1250°C, the $Na_2SiO_{3(l)}$ formed according to equation (**3**) below flows into the interlayer distances filling the pores exposing the sheets directly to the charge difference attractions that makes the structure more rigid.

$$Na_2O_{(s)} + SiO_{2(s)} \rightarrow Na_2SiO_{3(l)} \qquad \text{Equation (3)}$$

2.6.1.6 Loss on ignition

Loss on ignition (LOI) is widely used to estimate the amount of organic carbon and inorganic carbon in the soil (Dean, 1974). This method is based on differential thermal analysis in which organic matter begins to ignite at 200°C and burns out by 550°C (LOI_{550}) while most carbonate minerals that represent the inorganic carbon are destroyed at higher temperatures of 850°C for calcite and 750°C for dolomite depleting at LOI_{950} (Goldin, 1987). The calculation of the carbon matter burnt out of the sediment assumes that the ignition follows a stoichiometric relationship (Juan *et al.,* 2004). However some non carbon materials like phosphorus and sulphur in the sediments reduces the percentage of LOI by a small fraction if present.

2.6.2 Analytical instruments

There are a number of analytical instruments used in characterization of clay minerals. The instruments are selected according to need and availability. Some of the instruments used are:

2.6.2.1 X-Ray Diffractometry (XRD)

XRD disperses a crystal lattice using an x-ray beam and identifies the material by measuring the d-spacings and degrees, 2θ of diffracted x-ray beamaccording to Bragg's law, $2d\sin\theta=\lambda$ (Weitkamp *et al*., 2005). The diffracted x-ray beam is detected as a characteristic x-ray line on photographic plates. The measured line through Fourier Transform is compared to a catalogue of known substances.

However due to the irregular and complex nature of the clay mineral lattice especially in common clays XRD peaks do not resolve well. The collected data may substantially vary from sampled standards. It is therefore important to correlate the data received with an FTIR spectrum of the clay body.

2.6.2.2 Fourier Transform Infrared Spectroscopy (FTIR)

An IR radiation is passed through a sample from a glowing black-body source. Part of the radiation passes through while part is absorbed so long as the molecule has dipole moments. The irradiation causes vibrations, bending and/ or stretching of the molecular bonds whose frequencies are detected producing a spectrum that represents molecular absorption or transmittance as a unique molecular fingerprint. This analysis identifies materials through frequencies of their functional groups. The measured signal is

digitalized and sent to the computer where Fourier transformation takes place. This technique is nondestructive, is a high speed determination with increased sensitivity and measures all frequencies simultaneously due to the interferometer.

2.6.2.3 Energy Dispersive X-ray Spectroscopy (EDX)

Energy Dispersive X-ray spectroscopy relies on the interaction of the sample and some x-ray excitation. A high energy beam of electrons, protons or a beam of x-ray is focused onto a solid sample. The incident beam of electrons may excite and eject an electron from an inner energy shell creating an electron hole. An electron from a higher energy level relaxes to fill this hole emitting a characteristic x-ray that passes into Silicon or Lithium detector cooled at -200^{o}C using liquid nitrogen. The lines produced are analyzed for known samples and thickness gives the quantities as percentages.

CHAPTER THREE

MATERIALS AND METHODS

3.1 Study site

Ilesi in Kakamega County is situated on latitude 0.28° N and longitude 34.75°E. The study targeted three clay types and a grog sand used by the Ilesi potters in Shinyalu subcounty, 4 km south of Kakamega town, along the Kisumu to Kakamega road. Sugarcane baggase ash (SCBA) from Butali Sugar factory which is 20 kms north-east of Kakamega town was also collected and used in one of the mixtures in a bid to determine its possible inclusion in pottery. Figure 3.1 shows map of sites of study.

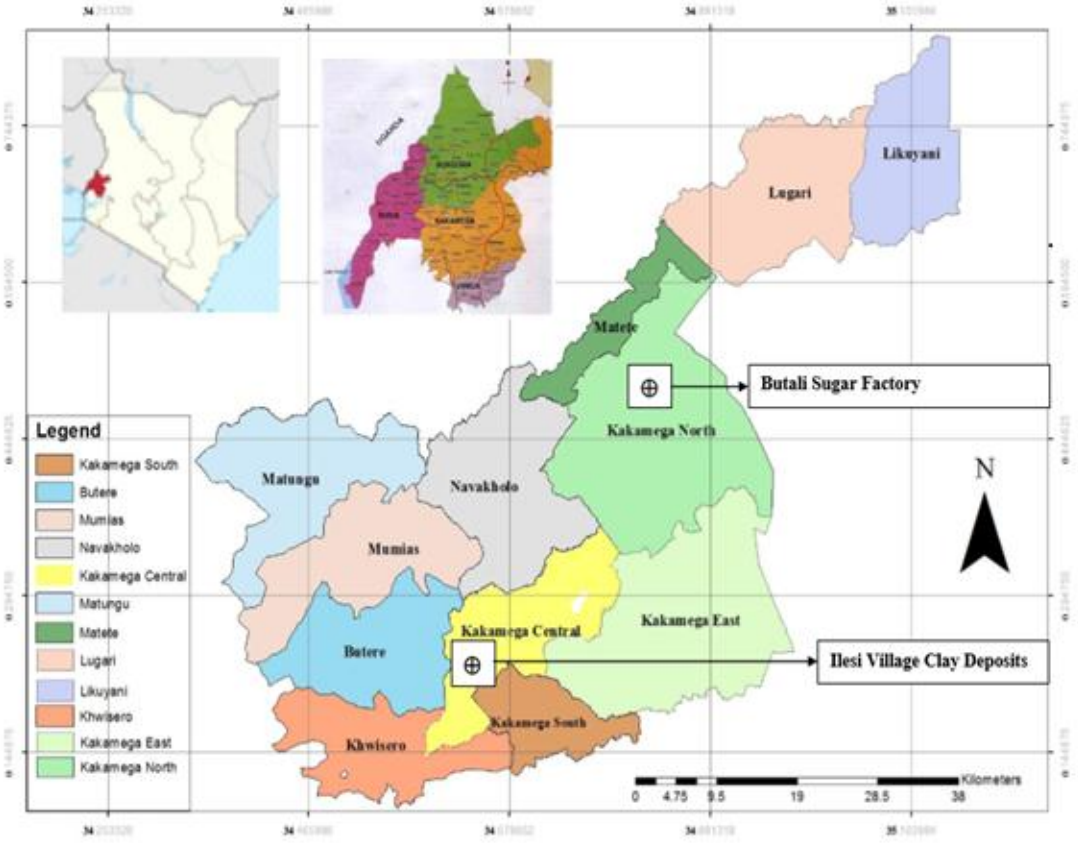

Figure 3.1: Map showing Ilesi clay deposit study site

3.2 Sample Collection and preparation.

Purposive sampling was used on the known Ilesi clay deposit sites (Christine, 2013). The area of about an acre along the swampy stream was marked with assistance of a member of the Ilesi traditional pottery. A pit measuring 1.5 meters by 1.5 meters square was dug on the site of black clay to a depth of 2.5 meters, surpassing the grey and the black sheets of soils. On this site the grey sheet lies on top of the black one. Using a spade and a shovel about 20 kg of the black soil from the black sheet was excavated from the sides of the pit. Similarly about 20 kg of the grey clay was excavated from its sheet.

The brown clay was removed from its marked site on the one acre square valley. A pit of about 1.5 meters by 1.5 meters square was dug using a shovel and spade up to a depth of about 1.5 meters. About 20 kg of brown soil was excavated using a shovel from the sides of the pit (Hesse, 1971).

The wet black, brown and grey clay soil samples and about 20 kgs of the Ilesi potters mixture were wrapped into clear polythene papers for transportation.

3.3 Pretreatment of samples

The wet clay samples collected from Ilesi deposits were broken by hand into small lumps and air-dried for two weeks.

3.3.1 Pretreatment for chemical characterization

Approximately 50g of each of the black, brown and grey dry clay samples were crushed using a wooden hammer. The crushed samples were sieved on 0.425 mm sieve and stored in clear polythene papers for the following spectroscopic analysis.

i) FTIR in which the infrared spectra were recorded on Nicolet Avatar 320 FTIR spectrometer, equipped with DTGS KBr detector.

ii) XRD was done on a Bruker XRD D2 Phaser.

iii) The clays were analyzed for their elemental composition by using a Shimadzu Ray EDX-800 HS.

The samples were used in chemical characterization as follows:

3.3.1.1 FTIR analysis

KBr pressed disc technique was used for preparing approximately 2g of the crushed clay solid sample. The 2g sample was put into the cell holder and inserted into the spectrometer. The spectrometer produced absorption and transmittance spectra for each clay.

3.3.1.2 XRD analysis

Approximately 2g sample was re-crushed into very fine powder then put into the cell holder and inserted into the spectrometer. The spectrometer produced diffractograms for each clay. The spectrometer's computer analyzed the difractrograms into percentage minerals.

3.3.1.3 EDX analysis

Approximately 2g sample was put into the cell holder and inserted into the EDX spectrometer. The spectrometer produced spectra for each clay. The spectrometer's computer analyzed the spectra into percentage elements as oxides.

3.3.2 Pretreatment for physical characterization

Approximately 500g of each of the clays namely, the black, brown and grey clays were crushed using a wooden hammer. The crushed samples were sieved on 0.425 mm sieve and stored in clear polythene bags for Atterberg limits determinations, loss on ignition and moisture content. Approximately 350g of dry clay lumps were put aside for the particle size test.

The remaining dry lumps of clay samples were crushed by KUD- Humboldt-Wedaq and sieved on 2 mm standard mesh in order to remove the gravel, rock and organic matter like humus, roots and stems. The soil that passed through the sieve was milled using Marina Torrential Super. The soil samples from the mill were sieved on 0.425 mm mesh and stored in dry polythene paper bags for determination of physical parameters of shrinkage, density, porosity and compressive strengths. Samples used in the determination of these physical properties were either cured or uncured. They were categorized as follows:

i) Uncured sieved raw clays were the black, brown, R1 and grey clays that were molded to plasticity and subjected to physical tests immediately.

ii) Cured sieved raw clays were clays and mixtures R2-R5 that were covered into plastic papers for 21 days after molding to plasticity before being tested for physical properties.

3.4 Physical parameter determination

The physical properties of the cured and uncured clay bodies of black, brown, grey were tested to determine the suitability of the raw clays and formulate recipes.

3.4.1 Determination of Atterberg limits

3.4.1.1 Liquid limit (ASTM D 4318)

This was done by the Cone Penetrometer Test (Rogers, 2006). Approximately 200g of the dry milled and sieved black sample was mixed with water on a flat glass plate using two metallic spatulas until plastic. A metallic cup was inverted and pressed into the molded sample hip. This was done carefully such as not to allow air into the sample. The cup with the wet clay was turned upright. A metallic spatula was used to level the clay in the cup. The metallic cup with the black clay body was put under the cone penetrometer. The cone was adjusted to the level of the clay in the cup. The gauge pointer was then adjusted to zero. The cone was released into the clay by pressing cone release button. The dial gauge was then adjusted to join the joining rod. A reading by the dial gauge when the rods join was recorded to give the penetration. The cone was removed and cleaned using damp piece of cloth. Approximately 35g of the sample from around the penetration region was removed from metallic cup. Approximately 5g from the 35g was set aside for the plastic limit determination while the remaining was put into another metallic cup and weighed as WM. The cup with approximately 30g sample was taken into an oven and dried for 24 hours at 110°C. It was removed after the 24 hours and weighed as DM. The moisture content was calculated from the equation (**4**) below:

$$\%\text{Moisture content} = \frac{(WM-DM)}{WM} \qquad \text{equation (4)}$$

where WM is Wet mass and DM, Dried mass.

The remaining sample on the mixing glass surface was adjusted using water or dry sample to achieve a penetration of between 15 and 22 mm. This test was repeated four times. At each penetration test, moisture content of the sample was determined by using equation (**4**) above. A graph of each penetration against its percentage moisture was plotted. This test was repeated for the brown and grey clay molds. Liquid limit was calibrated as percentage moisture at 20 mm penetration for each of the black, brown and grey clay bodies.

3.4.1.2 Plastic limit (ASTM D 4318)

The approximately 5g of the black clay body set aside in cone penetrometer test above was prepared for the plastic limit determination by adding dry sample powder or water until a desired plasticity. It was rolled into a thread of about 3mm in diameter on the glass plate it did not break into pieces. Small portions dry black clay soil were added to it and rolled again into threads of about 3mm until the pieces cracked. The cracked pieces were transferred into a metallic cup weighed as WM and then kept in an oven at 110°C for 24 hours to dry. The dry sample was weighed as DW. This was repeated 3 times. The plastic limit was calculated as percentage moisture content from the equation (**4**) on page 24. This test was repeated for the brown and grey clay bodies.

3.4.2 Particle size analysis

Approximately 350g of the 0.425mm crushed and sieved black clay sample was poured on a glass plate. Rocks and organic matter were removed by hand picking (Klinefelter and Hamlin, 1957). Approximately 250g of the remaining sample was shaken through a stack of registered sieves of 2mm, 1mm, 0.6mm, 0.425mm, 0.3mm, 0.212mm and 0.15mm using an electric shaker (Abolarin *et al.,* 2006; Barsom, 2003). The masses remaining on sieves 0.212 mm, 0.3mm, 0.425mm, 0.6mm, 1.0mm and 2 mm were taken and weighed to determine percent silt and sand by sieve analysis, ASTM D422. This was repeated for the brown and grey clay powders.

The sieved sample that passed through 0.212 mm sieve was analyzed for the clay content by the hydrometer ASTM 152H. This sample was mixed with 125 ml of 25% sodium hexametaphosphate solution, prepared by dissolving 40g sodium hexametaphosphate in 1000mL distilled water, to deflocculate the clay particles. The pretreated soil mixture was transferred into a 1000mL control cylinder and filled to the mark using deionized water. The hydrometer was dipped into the control/blank prepared by mixing 125 mL dispersing agent with deionized water to make 1000 mL solution. After reading the zero, the hydrometer was transferred into the sample placed in a 1000 mL cylinder. The meniscus level of the hydrometer was read after 30 seconds to give the clay and silt proportions. The hydrometer readings were repeated at 1, 2, 4, 8, 15, 30, 60, 120, 240 and 1440 minutes. The data collected was used to draw a graph from which the percent clay and silt were determined. The hydrometer test was repeated for the brown and grey clay samples.

3.4.3 Loss on ignition

Exactly 25g of milled and sieved black clay was dried in an oven at 110°C for 12 hours and put into a pre-weighed crucible, M_6 and weighed, M_4. The sample and crucible were heated in a kiln at 600°C for 6 hrs to burn out all carbon content. The sample was then cooled in a dessicator overnight to avoid absorption of moisture and weighed. Its mass was given as, M_5. The loss on ignition was calculated using equation (**5**) below. The procedure was repeated for the black clay at 800°C, and 1000°C, and for the brown and grey clays at 600°C, 800°C, and 1000°C to determine their carbon contents at varying calcinations temperatures.

$$\text{Loss on ignition} = \frac{(M_4 - M_5)}{(M_4 - M_6)} \times 100 \qquad \text{equation (5)}$$

3.4.4 Moisture content

Three clay blocks measuring 40mm long by 20mm wide by 20mm high were baked from molded uncured black clay. The blocks were put on pieces of aluminium paper and weighed to give wet weight as WW. They were dried in air for three weeks and in an oven for 24 hours at 110°C. The pieces were removed and immediately weighed with the aluminium paper to give dry weight as DW. The percentage moisture was calculated from equation (**6**) below.

$$\text{Percentage moisture} = \frac{(WW - DW)}{WW} \times 100 \qquad \text{Equation (6)}$$

The procedure was repeated for uncured brown, uncured grey, R1, cured black, cured brown and cured grey.

3.4.5 Shrinkage limits

Three blocks measuring 140mm long by 20mm wide and 20mm height were baked from the uncured black clay that had been molded to plasticity. Their lengths recorded as 140 mm. The pieces were left in the molding blocks for four days to dry. They were then removed and dried in air for two weeks. The pieces were then dried in the oven for 24 hrs at 110°C. Their lengths were measured and recorded as dry length, DL. They were fired in an oven at 600°C for six hrs and allowed to cool in the kiln. Their lengths were then measured in mm as Fired length, FL (Allen, 1986). The percentage shrinkage was calculated from the equations (**7**) and (**8**) below.

$$\% \text{ Linear dry shrinkage} = \frac{(WL-DL)}{WL} x100 \qquad \text{Equation (7)}$$

$$\% \text{ Linear fired shrinkage} = \frac{(WL- FL)}{WL} x100 \qquad \text{Equation (8)}$$

This procedure was repeated for the uncured black clay body at 800°Cand 1000°C. It was also repeated on similar blocks of uncured brown, uncured grey, potters mixture R1,cured black, cured brown, cured grey at 600° C, 800°Cand 1000°C.

3.4.6 Density

Twelve blocks measuring 40mm long by 20mm wide and 20mm height were molded from the uncured black clay. They were dried in air for two weeks, then in oven for 12 hours at 110°C. Three of the pieces were used to determine dry density. Each piece was weighed and immersed into kerosene in an overflow can. The volume of the displaced kerosene was measured. Three pieces were fired in a kiln at 600°C. They were then cooled in the oven until room temperature. Each of the pieces was weighed and its density determined using water in the overflow can. This procedure was repeated on 3

blocks fired at 800°Cand the last three fired at 1000°C. The procedure above was repeated for similar blocks of uncured brown, uncured grey, R1, cured black, cured brown and cured grey clays at 600°C, 800°C and 1000°C.

3.4.7 Porosity

The porosity of fired clay bodies was determined by Water Evaporation Method, WEM. Nine blocks measuring 40mm long by 20mm wide and 20mm height were baked from molded uncured black clay. The pieces were left to dry in the molding blocks for one week. They were removed and left to dry in air for another one week. They were then dried for 24 hours in an oven at 110°C. Three of the bone dry blocks were fired in a kiln to temperatures of 600°C, cooled in the oven at 110° C for 2 hrs after which they were transferred into desiccators to cool to room temperature. They were weighed as dry weight, WD. The three blocks were then boiled in water for half an hour, and then left soaked into the cold water for 15 hrs. They were removed from the water and wiped dry using a damp towel and weighed to get the wet weight, WW. Porosity was determined as percentage water absorbed using the equation (**9**) below.

$$\text{Porosity} = \frac{(WW - WD)}{WD} \times 100 \qquad \text{Equation (9)}$$

The above procedure was repeated on three blocks fired at 800°C and another three blocks kilned to 1000°C. Their porosities were determined using the equation (**9**).This procedure was repeated for uncured brown, uncured grey, R1, cured black, cured brown and cured grey clay bodies at 800°Cand 1000°C.

3.4.8 Compressive strengths

The green and fired compressive strengths of clay product were measured as fracture load (Klinefelter and Hamlin, 1957). Twelve blocks measuring 40mm long by 40mm wide and 40 mm height were made from the uncured black clay mold. The blocks were left in the molding blocks for one week to dry. They were then removed and dried for two weeks in air. The pieces were dried in the oven for 24 hrs at 110° C. The dry pieces were then subjected to fracture load using Universal compression and bending machine. Three other blocks were fired to 600°C in a kiln, cooled and subjected fracture load. Three others were fired to 800°C and subjected to fracture load. The last three were fired to 1000°C and subjected to fracture load. This procedure was repeated for the uncured brown, uncured grey, R1, cured black, cured brown and cured grey at green, 600°C, 800°C and 1000°C.

3.5 Recipe formulation

After chemical and physical characterization of the black, brown, grey clays and R1, a recipe used by Ilesi potters, mixtures R2 to R6 were developed by mixing the raw clays in optimized ratios. Quantities by percentage ratios of raw materials were measured accurately as shown in Table 3.1. A total of 5 kg of each mixture was molded to plasticity. For instance R2 was prepared by weighing 1000g black sieved clay, 1500g brown sieved, 1500g grey sieved and 1000g sieved grog sand. The masses for the ratios in R3 to R6 were determined in a similar manner. These mixtures were kept in polythene papers and stored for 21 days to cure. Table 3.1 shows the percentage ratios in the recipes of molded clay that was prepared for the analysis.

Table 3.1: Ratios of percentage raw materials by mass

Material used	Recipe					
	R 1	R 2	R 3	R 4	R 5	R 6
% Black clay	Approx.28	20	15	20	20	25
% Brown clay	Approx.28	30	20	30	40	30
% Grey clay	Approx.28	30	35	30	30	30
% Grog	Approx.16	20	30	0	5	15
% SCBA	0	0	0	20	5	0
% Total	100	100	100	100	100	100

SCBA is Sugar cane Bagasse Ash

These recipe formulations, R2 to R6 were tested on the physical parameters of shrinkage, density, porosity and compressive strength so as to establish the recipe that is most suitable for pottery.

3.5.1 Shrinkage limits

Three blocks measuring 140mm long by 20mm wide and 20mm height were molded to plasticity from R2. Their lengths recorded as 140 mm. The pieces were left in the molding blocks for four days to dry. They were then removed and dried in air for two weeks. The pieces were then dried in the oven for 24 hrs at 110°C. Their lengths were measured as dry length, DL. They were fired in an oven at 600°C for six hrs and allowed to cool in the kiln. Their lengths were then measured in mm as Fired length, FL (Allen, 1986). The percentage shrinkage was calculated from the equations (**7**) and (**8**) on page 27. This procedure was repeated for the R3, R4, R5 and R6 at 600°C. The shrinkage of R2, R3, R4, R5 and R6 was determined in the same manner at 800°Cand 1000°C.

3.5.2 Density

Twelve blocks measuring 40mm long by 20mm wide and 20mm height were molded from the R2 clay body. They were dried in air for two weeks, then in oven for 12 hours at

110°C. Three of the pieces were used to determine dry density. Each piece was weighed and immersed into kerosene in an overflow can. The volume of the displaced kerosene was measured. Three pieces were fired in a kiln at 600°C. They were transferred and cooled in the oven. Each of the pieces was weighed and its density determined using water in the overflow can. This procedure was repeated on 3 blocks fired at 800°C and the last three fired at 1000°C. The procedure above was repeated for similar blocks of R2, R3, R4, R5 and R6 at 600°C, 800°C and 1000°C.

3.5.3 Porosity

Nine blocks measuring 40mm long by 20mm wide and 20mm height were baked from molded R2. The pieces were left to dry in the molding blocks for one week. They were removed and left to dry in air for another one week. They were then dried for 24 hours in an oven at 110°C. Three of the bone dry blocks were fired in a kiln to temperatures of 600°C, cooled in the oven at 110° C for 2 hrs. They were then transferred into desiccators to cool to room temperature and weighed, WD. The three blocks were then boiled in water for half an hour, and then left soaked into the cold water for 15 hrs. They were removed from the water and wiped dry using a damp towel and weighed, WW. Porosity was determined as percentage water absorbed using the equation (**9**) on page 28. This procedure was repeated on three blocks of R2 fired at 800°C and another three blocks kilned to 1000°C. Their porosities were determined using the equation (**6**) on page 26. The procedure above was repeated for similar blocks of R3, R4, R5 and R6 at 600°C, 800°C and 1000°C.

3.5.4 Compressive strengths

Twelve blocks measuring 40mm long by 40mm long and 40 mm height were made from R2. The blocks were left in the molding blocks for one week to dry. They were then removed and dried for two weeks in air. The pieces were dried in the oven for 24 hrs at 110° C. Three of the dry pieces were then subjected to fracture load using Universal compression and bending machine. Three other blocks were fired to 600°C in a kiln, cooled and subjected fracture load. Three were fired to 800°C and subjected to fracture load. The last three were fired to 1000°C and subjected to fracture load. The procedure above was repeated for similar blocks of R2, R3, R4, R5 and R6 at 600°C, 800°C and 1000°C.

3.6 Losses

Losses were determined by identifying the number of blocks that showed swelling during forming and those that cracked during drying and firing during the shrinkage tests.

3.6.1.1 Swelling

Uncured black clay was molded to plasticity. The clay body was gently pressed into the shrinkage molding blocks placed on a flat table to form twelve 140mm long by 20mm wide and 20mm height blocks. The top of the mold for each sample was leveled using a metallic plate. The number of wet clay blocks that showed swelling on top were marked and recorded. This was repeated for the uncured brown, R1, uncured grey, cured black, cured brown, cured grey clay bodies, R2, R3, R4, R5 and R6.

3.6.1.2 Drying

Twelve blocks of the uncured black clay body measuring 140mm long by 40mm wide and 40mm height were prepared in the shrinkage wooden blocks and allowed to dry in air for 4 days. They were removed and dried in air for one week. They were put in an oven at 110°C for 24 hours. Those that showed cracking after being removed from the oven were counted and recorded. This was repeated for the uncured brown, R1, uncured grey, cured black, cured brown, cured grey clay bodies, R2, R3, R4, R5 and R6.

3.6.1.3 Firing

Twelve blocks of the uncured black measuring 140mm long by 40mm wide and 40mm height were prepared in the shrinkage wooden blocks and allowed to dry in air for 4 days. They were removed and dried in air for one week. They were put in an oven at 110°C for 24 hours. They were fired in a kiln at 600°C. The blocks of the clay bodies that cracked were counted and recorded. This was repeated at 800°C and 1000°C noting the number that cracked at each firing temperature. This was repeated for the uncured brown, R1, uncured grey, cured black, cured brown, cured grey clay bodies, R2, R3, R4, R5 and R6 at firing temperatures of 600°C, 800°C and 1000°C.

3.7 Data analysis

Atterberg limits data and sieve analysis were analyzed by regression analysis with linear graphs of cone penetration against the moisture content and curves of percentage finer against the particle diameter. Data on shrinkage, Loss on ignition, moisture content, porosity, compressive strengths and density was analyzed by Anova with relevant graphs.

CHAPTER FOUR

RESULTS AND DISCUSSION

4.1 Introduction

This study set out to determine the physical and chemical characteristics of the raw clays used for pottery by Ilesi potters. Three soil samples coloured black, brown and grey were collected and each was divided into two. One set was used without curing while the other was cured for 21 days before use for physical characterization. To gain insight into the causes of the losses incurred by the Ilesi potters, the soil samples and grog were mixed in different ratios (R2 to R6) and molded into blocks whose physical properties were determined and compared with those made from the recipe use by Ilesi potters, R1 (Table 4.1). Results on the physical properties of the cured and uncured black, brown and grey clays, Atterberg limits, particle size, loss on ignition, moisture content, shrinkage, compressive strengths, porosity and density are presented and discussed.

Table 4.1: Sample groups

1	2	3	4	5	6	7	8	9	10	11	12
Uncured black	Cured black	Uncured brown	Cured brown	Uncured grey	Cured grey	R1	R2	R3	R4	R5	R6

The data on mineralogy and elemental composition of the clays is presented in tables, spectra and compared with results obtained in studies from other areas.

4.2 Screening tests of raw clays

The black clay soil was found to be more uniform and rigid, with very few sand particles and organic matter like humus, roots and wood. Its milled sample was very powdery with

little crystalline particles. The brown and grey samples had coarse particles, transparent pieces of rock attributed to the high percent microcline at 42.6% and 44.6% respectively as seen in table 4.4. Both had a crystalline feel. Table 4.2 gives the soil profile of the clay deposits, their appearances and compositions in terms of percentage clay, silt and sand from the sieve analysis as in table 4.7.

Table 4.2: Profile description of clay soils from deposit depths when milled

Depth/m	**Sample**	**Description**	**% Clay+ silt**	**% Sand**
0.5-1.0	Grey	Dark-grey coarse, crystalline particles, humus, wooden sticks.	48	52
1.0-1.5	Brown	Reddish brown in grey, rough surface, transparent coarse, crystalline particles.	36	64
1.2-2.0	Black	Black, smooth and stone hard, fine powder.	62	38

4.3 Mineral and chemical composition of raw clays

The mineral composition of each of the three types of clays studied were determined by FTIR and correlated by powder x-ray diffraction. The chemical composition of the clays was determined by EDX and the results are presented and discussed below.

4.3.1 FTIR Spectroscopy

As the individual clays often occur in a form of mixed-layer clay minerals with various ratios of individual components, IR curves were recorded to confirm the clay mineral assemblage (Lenka and Eva, 2005). Usually analysis of kaolins using KBr pellet gives two strong bands at 3800 cm^{-1} and 3600 cm^{-1} attributed to OH stretching vibrations of adsorbed water and a weakly segregated doublet at 1080 cm^{-1} and 1020 cm^{-1} in the finger

print region representing Si-O and Al-OH stretching respectively (Tan, 2011). The spectrum for black clay is given in figure 4.1 below.

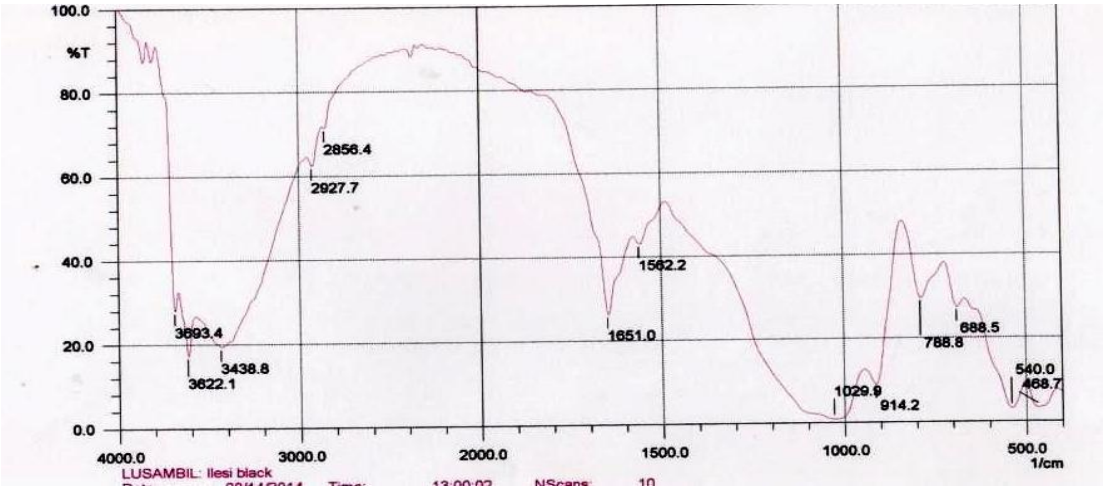

Figure 4.1: FTIR spectrum for black clay

The bands at 3693.4 cm^{-1} and 3622.1 cm^{-1} in figure 4.1 are attributable to the octahedral OH stretching in dickite. The bands at 1029.9 cm^{-1}, 788.8 cm^{-1}, 688.5 cm^{-1} in the fingerprint region could be due to the tetrahedral Si-O-Si and Si-O stretching while the peaks at 540.0 cm^{-1} and 468.7 cm^{-1} can be attributed to the Si-O deformation (Abuh *et al*., 2014). Figure 4.2 shows the FTIR spectrum of the brown clay.

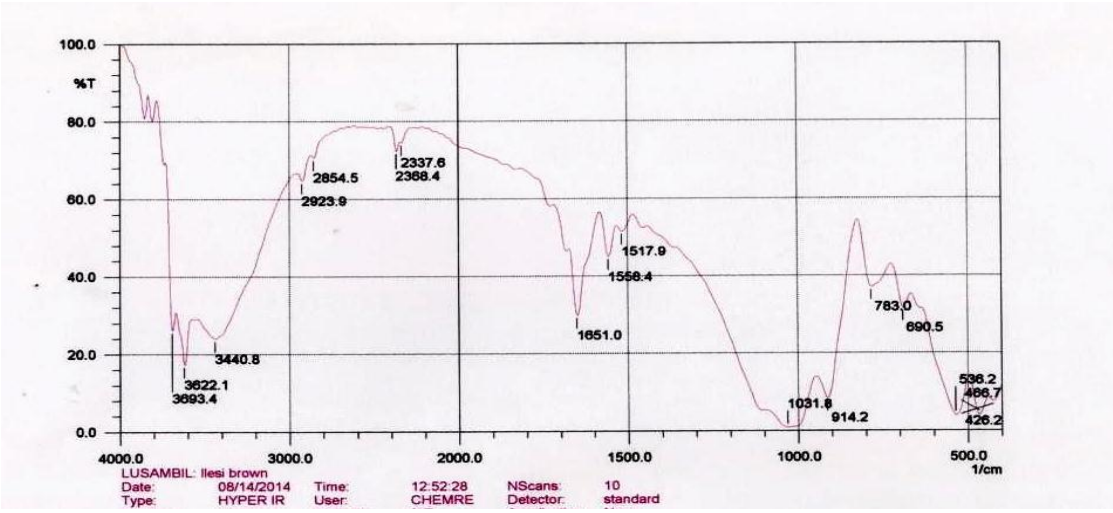

Figure 4.2: FTIR spectrum for brown clay

The bands at 3693.4 cm^{-1} and 3622.1 cm^{-1} in figure 4.2 are attributable to the octahedral OH stretching in the dickite. The bands at 1031.8 cm^{-1},783.0 cm^{-1}, 690.5 cm^{-1} in the fingerprint region could be due to the tetrahedral Si-O-Si and Si-O stretching. The bands 536.2 cm^{-1} and 466.7 cm^{-1} could be due to the Si-O deformation. The band seen at 914.2 cm^{-1} in the fingerprint region can be attributed to the octahedral Al-O-H stretching. Figure 4.3 shows the FTIR spectrum of the grey clay.

Figure 4.3: FTIR spectrum for grey clay

The grey clay in figure 4.3 has peaks seen at 3435.0 cm^{-1} and 1651 cm^{-1}that can be assigned to the H-O-H stretch of free water or water bound by hydrogen bonding. The bands at 3693.4 cm^{-1} and 3622.1 cm^{-1} may be due to the octahedral OH stretching in the dickite with the band at 1031.8 cm^{-1} in the fingerprint region being for the Al-O-H stretching. The bands at 1031.8 cm^{-1}, 781.1 cm^{-1}, 690.5 cm^{-1} in the fingerprint region can be attributed to the tetrahedral Si-O-Si and Si-O stretching. The bands at 536.2 cm^{-1} and 466.7 $cm^{-1}$are attributed to Si-O deformation. The spectra for the black, brown and grey clays are similar and their analysis point to a sample of a clay mineral with dickite, alkali feldspars and quartz as summarized below.

4.3.1.1 Dickite

The IR spectra of kaolins showed a doublet at 3696 cm^{-1} and 3620 cm^{-1}. The doublet at 3693.4 cm^{-1} and 3622.1 cm^{-1} in figures 4.1, 4.2 and 4.3 can then be attributed to dickite Al-O-H stretching whose fingerprint region showed bands for the same stretching at 1029.9 cm^{-1} in figure 4.1 and 1031.8 cm^{-1} in figures 4.2 and 4.3. In baseline studies on kaolinite FTIR bands were seen at 3694 cm^{-1}, 3620cm^{-1} and 1033 cm^{-1} (Jana and Peter, 2001). These bands are similar to the peaks obtained for the Ilesi clays.

4.3.1.2 Albite and Microcline

Feldspars have fingerprint region in 1150-1000 cm^{-1}. Therefore the bands at 1031.8cm^{-1} in figures 4.5 and 4.6 and 1029.9 cm^{-1} in figure 4.4 are then attributed to Si-O-Si stretching. The bands at 690.5 cm^{-1} in figures 4.2 and 4.6, 688.5 cm^{-1} in figure 4.1, 540.0 cm^{-1} in figure 4.1, 536.2 cm^{-1} in figures 4.2 and 4.3 confirm Si-O-Al stretching in the feldspars. These spectra are similar to those of the research on central Bosnia clays (Jovanovic and Mujkanovic, 2013).

4.3.1.3 Quartz

Quartz has fingerprint bands at 1100 cm^{-1}, 800 cm^{-1}, 500 cm^{-1}. Therefore the bands at 1031.8 cm^{-1} in figures 4.2 and 4.3, 1029.9 cm^{-1} in figure 4.4 are therefore attributed to Si-O-Si stretching. The bands at 788.8 cm^{-1} in figure 4.1, 783 cm^{-1} in figure 4.5 and 781.1 cm^{-1} in figure 4.3 are due to Si-O stretching while 468.7 cm^{-1} point to Si-O deformation (Abuh *et al*., 2014). The slight variations of the bands from those given in literature indicate the complex nature of bonding in clay minerals. Table 4.3 shows the close

comparison of spectral bands for the Ilesi clays alongside those recorded in a different research (Preeti and Singh, 2007).

Table 4.3: Spectral bands and their assignments

Black/cm^{-1}	Brown / cm^{-1}	Grey/cm^{-1}	Preeti's Clay/ cm^{-1}	Assignments
3693.4	3693.4	3693.4	3696.7	Al-O-H stretching
3622.1	3622.1	3622.1	3622.5	Al-O-H (inter octahedral) stretching
3438.8	3440.8	3435.0	3450.4	H-O-H stretching
1651	1651.0	1651.0	1633.4	H-O-H stretching
1029.9	1031.8	1031.8	1033.3	Si-O-Si stretching, Si-O-, stretching
914.2	914.2	914.2	914.5	Al-O-H, stretching
788.8	783.0	781.1	790.9	Si-O-, stretch., Si-O-Al, Si-O-(Mg,Al stretching
688.5	690.5	690.5	693.4	Si-O-, stretching Si-O-Al, stretching
540.0	536.2	536.2	538.4	Si-O-, stretching Si-O-Al, stretching
468.7	466.7	466.7	468.9	Si-O- stretching, Si-O-Fe stretching

4.3.2 X-Ray Diffraction (XRD)

It shows that the clays analyzed contained dickite, $Al_4Si_4O_{10}$ $(OH)_8$, albite, $NaAlSi_3O_{10}$, microcline, $KAlSi_3O_8$, and quartz, SiO_2 as shown in table 4.4.

Table 4.4: XRD data for the clay samples

Clay name	%Albite	% Dickite	%Microcline	%Quartz
Black	22.4	15.8	38.2	23.6
Brown	16.1	6.4	42.6	34.8
Grey	15.6	7.3	44.6	32.5

The clay soils analyzed had the same mineral assemblage since they were removed from the same valley. Albite and microcline are alkali feldspar fluxes while quartz is filler as well as a glassing material in pottery production. The results showed that the black clay has the highest percentage dickite and albite content of 15.8%, and 22.4%, respectively. The brown and grey clays have lower amounts of the dickite mineral 6.4% and 7.3%, respectively but high values for quartz, 34.8% and 32.5% again respectively. Therefore, these results showed that the black clay would be best suited for pottery than the brown

and grey clays. However, the physical properties of raw clays make it necessary to have the clays mixed into mixtures (Kent, 2008). For example, this black clay was sticky and difficult to achieve plasticity. XRD's diffracted x-ray beam from the clay sample is detected as a characteristic x-ray line on photographic plates whose intensity registers as peaks against their phase angle **(**Katherine and Benjamin, 1996). Figure 4.4 shows the diffractogram of the black clay.

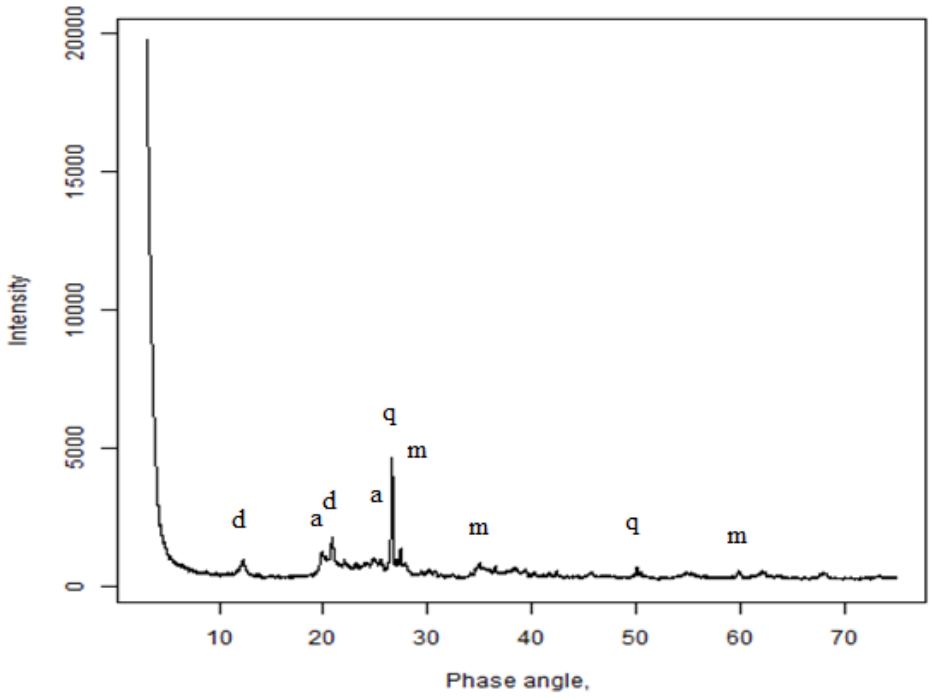

Figure 4.4:X-Ray Diffractogram for black clay

Key:d represents dickite, a , albite, m, microcline and q, quartz.

Kaolinite exhibits a characteristic first order diffraction peak at 2θ, 12.4°corresponding to a d-spacing of 0.713 nm and a second order diffraction at 2θ, 25° corresponding to a d-spacing 0.356 nm (Tan, 2011). The peaks observed and labeled in figure 4.4 represented the dickite, albite and microcline feldspars found normally in the region d-spacing of

0.630-0.645 nm and 0.310-0.325 nm (Tan, 2011) and quartz. Figure 4.5 shows the diffractogram for the brown clay.

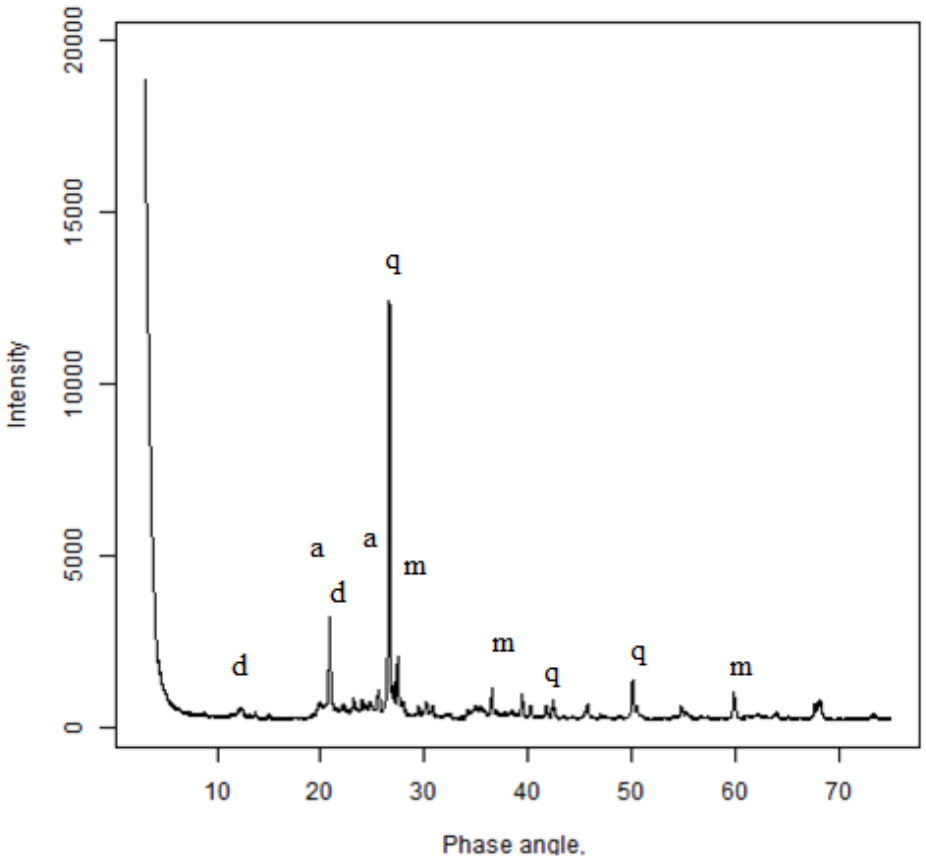

Figure 4.5: X-Ray diffractogram for brown clay soil

Key: d represents dickite, a, albite, m, microcline and q, quartz.

Like in the black clay, peaks identified in figure 4.5 are for dickite, quartz, albite and microcline. This shows that the mineral assemblage in brown clay is the same as in black except for the quantities. Figure 4.6 shows the diffractogram of the grey clay.

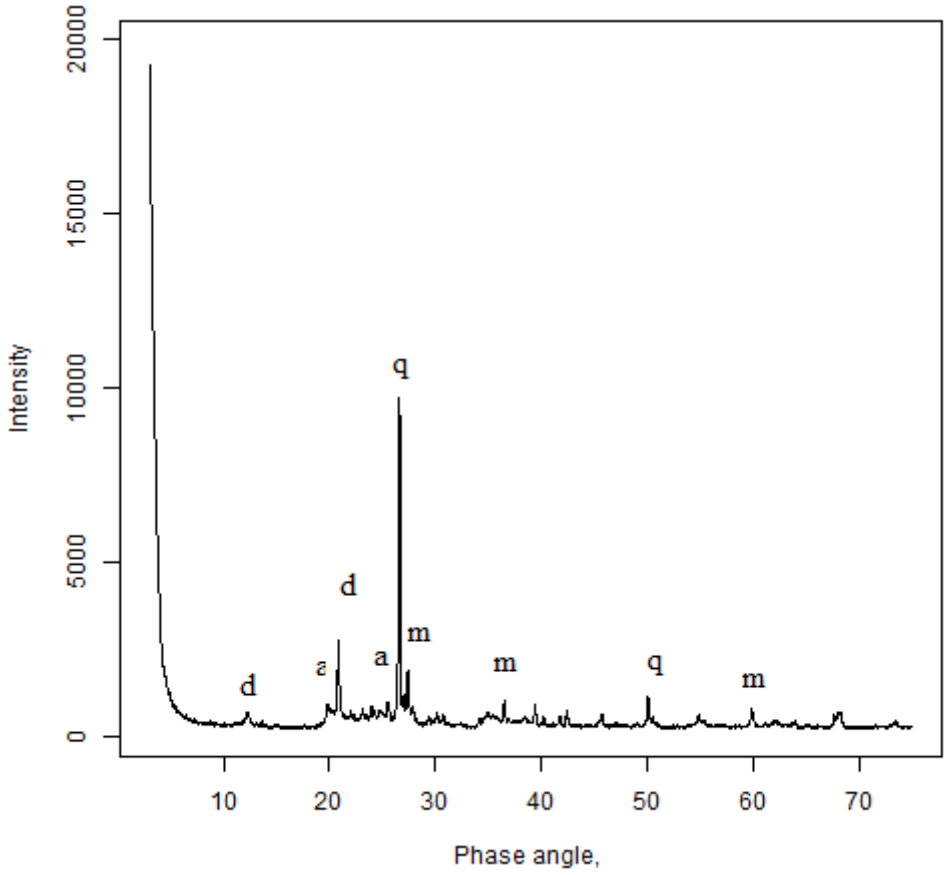

Figure 4.6: X-Ray Diffractogram for grey clay

Key: d represents dickite, a, albite, m, microcline and q, quartz.

The peaks for grey clay in figure 4.6 were at the same phase angles as in the black and brown showing presence of dickite, quartz, albite and microcline.

Generally figures 4.4, 4.5 and 4.6 showed dickite peaks are at 2θ, 12.4° and 21.5°, albite at 2θ, 22° and 28°, microcline at 2θ, 27.4° and 35° while quartz at 2θ, 21° and 26.9° (Osabar *et al*., 2009). The only difference noted between the clays is in the intensities of the diffractograms. These peaks are poorly resolved, due to the variable compositions and

degree of crystallinity that causes mutual interference with the diffraction patterns analysis (Ronald, 1967).

The data showed that iron is not in the clays as a mineral which would mean that all the iron in the clay body is lying in the interlayer distances as accessory ion. On average the accessory minerals are in very small percentages to show on diffractograms. The Ilesi clay mineralogy results are similar with those of other deposits like research on mineralogy of local clays in a Saudi Arabia (Mohsen and El-maghraby, 2010) and that done on central Bosnia clays (Jovanovic and Mujkanovic, 2013).

4.3.3 EDX spectroscopy

The results of element analysis as oxides are shown in the table 4.5.

Table 4.5: Percentage oxides of raw materials

% Elements	Black ±SE	Brown ±SE	Grey ±SE	Sand ±SE
SiO_2	64.94±0.614	63.86±0.607	67.50±0.557	51.18±0.684
Al_2O_3	20.70±0.822	21.48±0.846	19.67±0.732	24.20±1.102
Fe_2O_3	7.56±0.034	7.40±0.034	4.76±0.026	16.49±0.057
K_2O	2.91±0.028	5.92±0.037	4.80±0.031	3.73±0.035
CaO	1.49±0.018	0.23±0.050	1.07±0.015	1.36±0.021
TiO_2	1.42±0.033	1.04±0.030	1.26±0.032	1.62±0.039
SO_3	0.91±0.047	0.00	0.64±0.033	1.00±0.051
SrO	0.05±0.001	0.05±0.001	0.04±0.001	0.10±0.002
Rb_2O	0.02±0.001	0.03±0.001	0.03±0.001	0.050±0.002

N.B: mean±sd (n = 3), black=Ilesi black, brown= Ilesi brown, Grey =Ilesi grey.

Table 4.5 shows that the major components in the samples were SiO_2, Al_2O_3 and Fe_2O_3. The SiO_2 composition ranged between 63.86%-67.5%, Al_2O_3, 19.67%-21.48% and Fe_2O_3, 4.76%-7.56%. This data is similar to research on chemical composition of different clays and pure kaolin in Saudi Arabia (Mohsen and El-Maghraly, 2010), common clays of Yola Bentoni in Nigeria (James *et al.,* 2008) and Adiabo clays in

Nigeria (Abuh *et al.,* 2004), clays in Odupani in South eastern Nigeria (Osabar *et al*., 2009).

The percentage of MgO is below detection level. These clays should not expand during drying which can cause cracking (Kirk and Othmer, 2004). The percentage of CaO from table 4.5 is low, that is between 0.23±0.050% and 1.49±0.018% which suggests that these clays should not have swelling properties (Kirk and Othmer, 2004). This rules out the nature of the clays being responsible for the cracking during drying and firing by the potters at Ilesi. This is confirmed by the XRD data from table 4.4 that shows absence of bentonites, calcite and dolomite.

Although the clays are missing Na_2O, the percentage composition of albite in table 4.4 serves well for glass formation during the firing process. The data on table 4.5 also shows a ratio of silica: alumina to be 3:1 (Folorunso *et al.,* 2014) for the black, brown and grey clays suggesting that these clays can also be used to manufacture synthetic zeolite (Nwosu, 2013).

Iron (III) oxide at 7.56%, 7.4%, 4.76% and 16.49% in black, brown, grey and sand respectively gives red colour to fired pots especially in those mixtures with high percentage of the brown clays. In addition they also act as fluxes during the sintering process. These iron (III) oxide levels are however too high for high quality ceramic products like bathroom tiles that require below 1% iron oxide (Olale, 1985). If a wet beneficiation method mixed with dilute acid is used in the clay body pretreatment, then

the clay would reduce the percentage of this iron and other elements like calcium and titanium making it suitable for production of these tiles (Karoki, 2008).

The amount of K_2O is higher in the grey, 4.8%, than the black, 2.91%, due to the higher percentage microcline feldspar, 44.6% as seen in table 4.2 which yields the free K_2O during the hydrothermal alteration according to the equation (**1**) on page 5.

4.4 The Physical Properties of the Ilesi Clays

The properties determined in this study include plasticity index, particle size, loss on ignition, moisture content, linear shrinkage, densities, porosity and compressive strengths.

4.4.1 Plasticity index

It was generally recognized that fall cone tests were difficult to perform at water contents near the plastic limit since the soil samples are stiff and difficult to mix (Feng, 2000; Stone and Phan, 1995). Figure 4.7 shows the best of fit lines from these penetrometer results for the three clay samples.

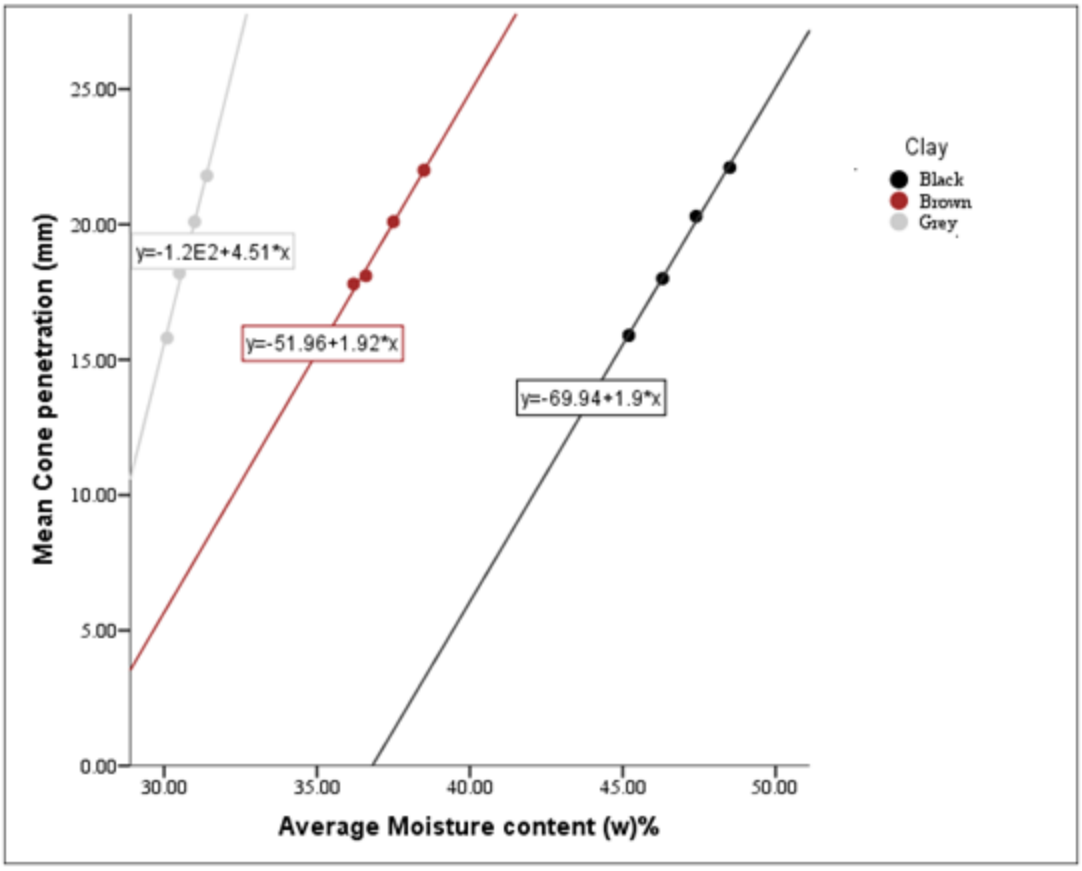

Figure 4.7: Penetration against moisture content for the black, brown and grey clays

The liquid limits are calculated from the line equations in figure 4.7 at mean penetrometer value of 20mm as follows:

Black clay	Brown clay	Grey clay
Y= -69.94+1.9x 1.9x=20+69.94 X = 47.34%	y = -51.96+1.92x 1.92x =20+51.96 x = 37.48%	$y=-1.2x10^{2}+4.51x$ 4.51x =20 + 120 x = 31.04%

Table 4.6 shows the plasticity index (PI) values.

Table 4.6: Atterberg limits for the black, brown and grey soils

Clay soil	BLACK	GREY	BROWN
Liquid Limit(% L.L)	47.34	31.04	37.48
Plastic Limit% (PL)	28.80	21.50	20.00
Plasticity index(P.I)	18.54	9.54	17.48

These limits, P.I=L.L-P.L indicate the workability of clay in terms of compressibility, permeability and strength (Thomas, 1998). A plasticity index of above 15 is suitable for pot making as discussed in the introduction. Such a clay body offers larger room for workability during the forming stage. Therefore the black clay with a PI of 18.54 has a better range for workability while the grey one has the lowest with 9.54. This is due to the fact that the black clay has a higher percentage of small size particles at 62% that readily absorb water while grey has small percentage of small size particles with 48% as shown in table 4.7. The grey clay found the valley collects more organic matter that increases its plasticity than the brown. Table 4.2 confirms this since organic matter was seen in this grey soil profile. The clay soils named as black, brown and grey have sufficient plasticity for molding hence suitable for formation of pot products with a liquid limit of above 25% and a plastic limit of above 20% as seen in table 4.6.

These results compare closely with research results on red clay soils at Arboretum, Nairobi (Wanyonyi, 2004). Similar results were obtained for soils in Uganda (Mugagga *et al.,* 2010). The liquid limit and plastic limit results of the Ilesi clays in table 4.6 are also similar to those determined for Makondeni clays in South Africa (Amponsah-Dacosta *et al.,* 2013).

4.4.2 Particle size analysis

Sieve analysis is used for determination of sand fraction while hydrometer tests determines the silt and clay fractions since sieves of small diameters like 0.02mm and below are not available. Figure 4.8 shows the graph for particle size of black clay.

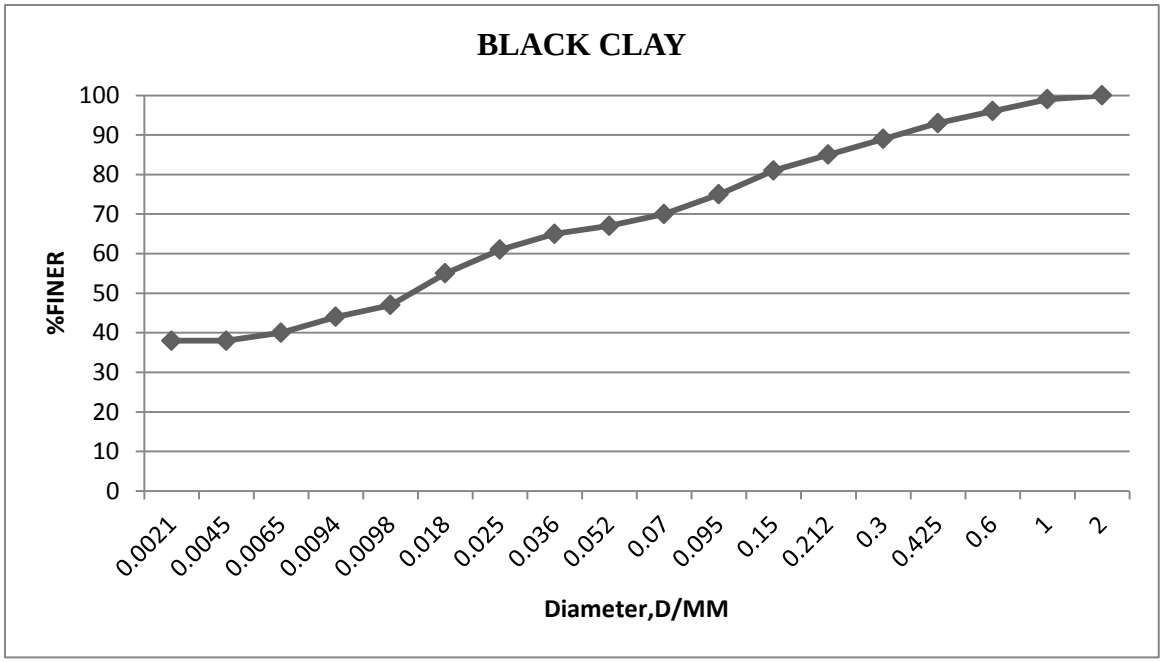

Figure 4.8: Percentage particles against diameter/mm for black soil

N.B:Particle Size Analysis(PSA) standard scale
Clay = < 0.002 mm, Silt = 0.002-0.02 mm, Fine sand = 0.02-0.2 mm, Coarse sand = 0.2-2 mm, Gravel = > 2mm.

The standard sieve shaker was used to isolate the 240 g black clay that passed through the 2mm sieve because the interest on the soil texture was only with clay, silt and sand. Some of the amount of sand between 0.02- 2mm diameter was calculated from the shaker but some pass through the 0.15mm sieve and was measured by gravity concentration by the hydrometer. Analysis of drawn graph of figure 4.8 showed that <0.002 was equivalent to 38% which represents the clay fraction. In addition the drawn graph showed that 0.02 mm point was equivalent to 62%. Therefore 62% minus 38% gives 24% which represents the fraction of silt. If clay and silt is 62% then 0.02mm to 2mm equals 38% which represents the whole sand fraction. Figure 4.9 shows the particle size graph for brown clay.

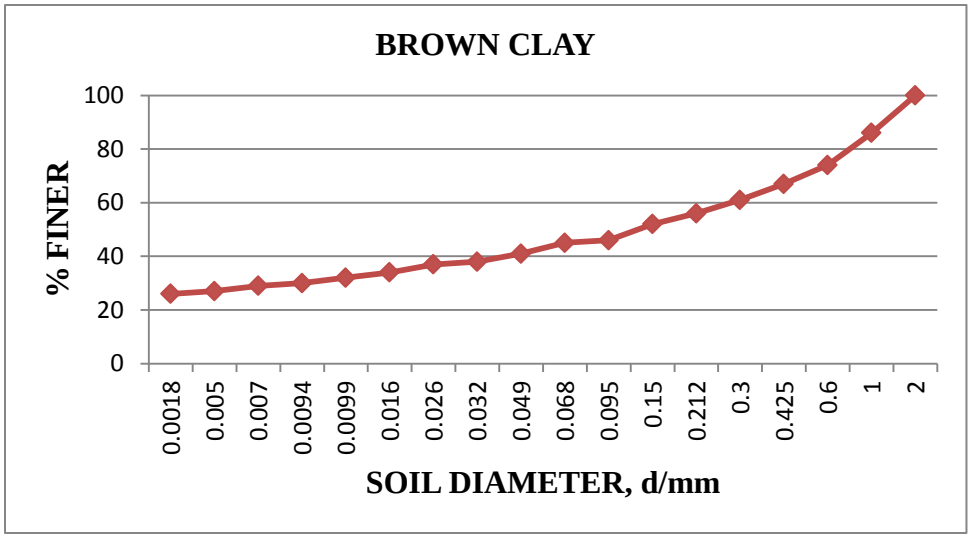

Figure 4.9: Percentage particles against diameter/mm for brown soil

N.B: Particle Size Analysis (PSA) standard scale
Clay = < 0.002 mm, Silt = 0.002-0.02 mm, Fine sand = 0.02-0.2 mm, Coarse sand = 0.2-2 mm, Gravel > 2mm

245g of the brown soil texture is computed in the same manner from the graph of the sieve analysis and the hydrometer readings. Some of the sand between 0.02 and 2mm in diameter passed through the 0.15mm sieve and was measured by gravity concentration. Therefore an analysis of drawn graph of figure 4.9 was used to calculate the soil texture. The graph showed that 26% of the particles have diameter < 0.002 corresponding to clay fraction and a calibration for 0.02 mm diameter was at 36% hence silt content of 36% minus 26% which gives 10%. The remainder percent, 64% represents sand. Figure 4.10 shows the particle size graph for grey clay.

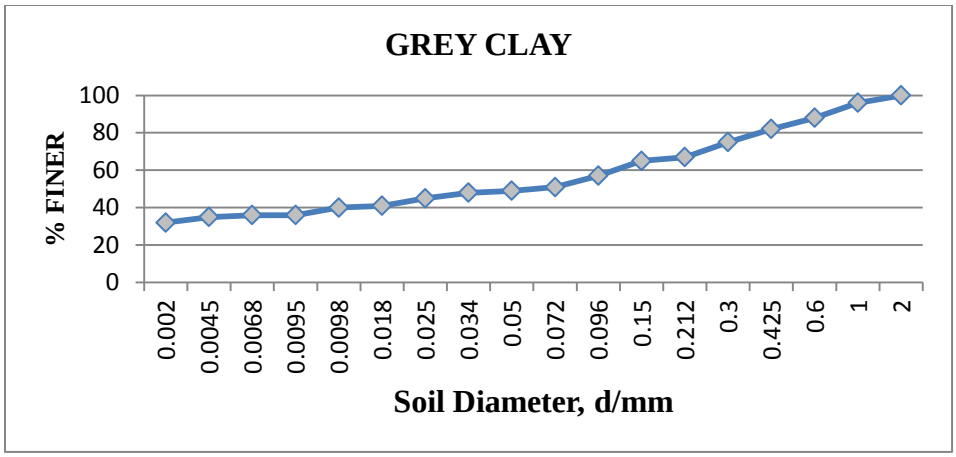

Figure 4.10: Percentage particles against diameter/mm for grey soil

N.B: Particle Size Analysis (PSA) standard scale
Clay = < 0.002 mm, Silt = 0.002-0.02 mm, Fine sand = 0.02-0.2 mm, Coarse sand = 0.2-2 mm, Gravel > 2mm.

245g of the soil texture for the grey clay was calculated in a similar manner to the black and brown. Analysis of drawn graph in figure 4.10 showed that <0.002 equated to 32% clay fraction, 0.02 mm diameter calibrates to 48% which calculated to a silt content of 16%. The remaining portion of 52% represented the whole sand fraction of 0.02 to 2mm. The collected data was summarized into table 4.7 of soil texture.

Table 4.7: Soil texture

Clay Body	% CLAY	% SILT	% SAND
Black	38	24	38
Brown	26	10	64
Grey	32	16	52

The sieve analysis shows that black clay has highest percentage clay content with 38% followed by the grey, 32% and lastly brown, 26%. This means the black clay will have a higher plasticity index as corroborated with 18.54 in table 4.6. The brown clay with clay content 26% has a plasticity index of 17.48 which is lower than of black. However the

grey clay which was seen to have larger proportion organic matter as shown by table 4.2 quickly traps moisture achieving a liquid limit quickly which reduces its plastic limit (Teixeira *et al.*, 2001).

The particle size is important in explaining the physical and chemical properties of a clay body. With the same minerals present in the Ilesi clays, the difference in their properties depends largely on the particle size and effects of the interlayer forces (Vanorio *et al.*, 2003). This is why there should be a delicate balancing act when it comes to formulation of working clay recipes.

4.4.3 Loss on ignition

Loss on ignition, LOI is the decrease in mass of a sample when it is heated and was determined in a kiln. The decrease arises from the burning out of the organic matter both as humus and carbon content. LOI_{550} assumes that all water in the soil sample has evaporated out by 550°C. Table 4.8 shows the loss on ignition at varying temperatures.

Table 4.8: Loss on ignition

	%Mean loss on Ignition **±SE**			
Claybody	600°C	800°C	1000°C	P-value
Black	6.08±0.23^{a}	8.28±0.04^{b}	11.00±0.21^{Bc}	<0.001
Brown	6.15±0.18	7.52±0.83	7.17±0.23^{A}	0.218
Grey	6.56±0.22	7.72±0.46	7.76±0.07^{A}	0.067
P-value	0.294	0.620	<0.001	

N.B: Mean values followed by the same capital letter(s) within the same column do not differ significantly from one another while mean values followed by the same small letter(s) within the same row do not differ significantly from one another (α=0.05, one-way ANOVA, SNK-test).

One-way Anova showed that there were significant differences in loss on ignition of the black clay and between different clay bodies fired at 1000°C.

The loss on ignition at 600°C showed that the grey soil had the highest LOI of 6.56% due to the organic matter as shown by table 4.2 while the black had the lowest at 6.08%.The black clay showed higher values of LOI at 800°C and 1000°C. This could be because of low aerobic degradation which is caused by the inability of this soil to allow in oxygen due to its very fine texture and also high percentage of inorganic carbon. The values at 1000°C of 6.76% for the grey soil and 7.17% for the brown soil are not significantly different since they are found within similar depth profile as seen in table 4.2 and have similar particle size soils as shown in table 4.7.

A low loss on ignition of below 15% indicates that the clay has lower carbonaceous matter and higher mineral matter content (Juan *et al.,* 2004; Preeti and Singh, 2007). From this data of between 6.08% and 11.00%, the Ilesi clays have low carbon content. Therefore all the clays have above 88% mineral content which makes the clays suitable for a range of products. In addition the texture of the clay body does not change much on firing. It is important to know organic matter concentration because it will burn during ceramics firing process resulting in mass loss, pore formation and reduction in density (Teixeira *et al.,* 2001).

4.4.4 Moisture Content

Moisture content of clay is the maximum amount of water that a plastic clay body can hold. The moisture values for clay bodies from Ilesi clays are given in table 4.9.

Table 4.9: Percentage Moisture content

Claybody	**%(Mean±SE)**
Black	38.82 ± 0.12^{d}
Brown	25.03 ± 0.16^{a}
Grey	30.91 ± 0.06^{c}
R1	26.00 ± 0.19^{ab}
R2	28.91 ± 0.10^{bc}
R3	27.82 ± 0.05^{abc}
R4	42.35 ± 0.11^{e}
R5	36.06 ± 0.56^{d}
R6	30.53 ± 2.75^{c}
p-value	<0.001

N.B:Mean values followed by the same small letter(s) within the same column do not differ significantly from one another (α=0.05, one-way ANOVA, SNK-test).

The black clay body had the largest moisture absorption of 38.82±0.12% followed by the grey with 30.91±0.06% and brown with 25.03±0.16%. The data correlates with that done on Ugandan clays (Kirabira, 2003). The high moisture content may be attributed to the clay particle size. The small particle sizes in the black clay body offer large surface area for voids which increases moisture trapping as compared to brown which has large percentage of crystalline particles.

The black clay with the highest moisture content 38.82±0.12% has the highest plasticity index of 18.54 among the clay bodies. Clays' surface adsorbs water which holds the sheets together by surface tension forces and when these forces have been overcome by excess water the clay body to flows easily (Olubayode *et al*., 2015). Fine grained clays like Ilesi black 62% clay and silt as shown in table 4.2 have much more affinity for water and therefore exhibit higher plasticity. This black clay would improve the plasticity index of the grey clay from the 9.54%, if the two are mixed. This is the basis on which potters make recipes. Curing and mixing in suitable proportions of clays, evenly distributing the

moisture and reducing bubble content improves plasticity and optimizes the clay body's workability (Rusovich-Yugai and Neklyudova, 2007).

R4 registered the highest moisture content of 42.35±0.11% followed by R5 with 36.06±0.56% due to the effect of 20% SCBA in R4 and 5% SCBA in R5. SCBA traps moisture due to increased surface area in the clay bodies (Olubayode *et al*., 2015). The R1 had the smallest water content due to the high percentage sand and gravel. This is not significantly different from R2 and R3 at 28.91±0.10% and 27.82±0.05% respectively. The high percentage black clay of 25% in R6 as shown in table 3.1 is well compensated by the low percentage grog sand of 15% thus registers a modest moisture content of 30.53±2.75%.

4.4.5 Linear shrinkage

Clays shrink when they dry and when fired. The shrinkage limit is the water content where further loss of moisture will not result in any more volume reduction. The shrinking property of a clay body is characteristic to the clay and depends largely on the layer charge on the clay mineral and size of clay particles. The clays that have very large dry and fired shrinkage often crack during the drying and firing stage. Table 4.10 gives the percentage linear shrinkage values for the clays and their mixtures.

The cured clay bodies showed lower dry shrinkage than the uncured ones. For example, it can be seen from table 4.10 that uncured grey clay showed a linear shrinkage of 6.67±0.24% while that of the cured grey clay was 5.71%. Curing distributes the moisture uniformly into the clay particles thus developing strong hydrogen bonds which reduces

contraction when free moisture evaporates. Clays containing smaller particles like black with 62% clay and silt, shrink more than large sized particles like brown clays (36% clay and silt).

Table 4.10: Linear dry and fired shrinkage from pure clays and clay mixtures

Clay body	Dry (Mean±SE)% shrinkage	600°C (Mean±SE)% shrinkage	800°C (Mean±SE)% shrinkage	1000°C (Mean±SE)% shrinkage	p-value
BlackUncured	9.76 ± 0.24^{Ga}	10.48 ± 0.24^{Db}	10.71 ± 0.00^{Db}	13.10 ± 0.24^{Fc}	<0.001
BlackCured	9.52 ± 0.24^{Ga}	10.24 ± 0.24^{Da}	10.48 ± 0.24^{Da}	10.48 ± 0.24^{Da}	<0.001
Brown Uncured	7.62 ± 0.24^{Fa}	7.62 ± 0.24^{Bca}	8.33 ± 0.24^{Bca}	9.52 ± 0.24^{CDb}	<0.001
Brown Cured	6.19 ± 0.24^{ABCa}	7.38 ± 0.24^{BCb}	8.33 ± 0.24^{BCc}	8.57 ± 0.41^{BCc}	<0.001
Grey uncured	6.67 ± 0.24^{CDE}	6.90 ± 0.24^{BC}	7.38 ± 0.24^{ABC}	7.38 ± 0.24^{A}	0.160
Grey cured	5.71 ± 0.00^{Aba}	6.90 ± 0.48^{BCb}	8.57 ± 0.00^{Cc}	8.81 ± 0.24^{BCDc}	<0.001
R1	5.48 ± 0.24^{Aa}	6.67 ± 0.24^{Bb}	6.90 ± 0.24^{Ab}	7.38 ± 0.24^{Ab}	0.003
R2	7.38 ± 0.24^{EF}	7.62 ± 0.24^{BC}	7.14 ± 0.41^{AB}	7.86 ± 0.00^{AB}	0.330
R3	6.43 ± 0.00^{BCDa}	7.14 ± 0.41^{Bcab}	7.62 ± 0.24^{ABCbc}	8.33 ± 0.24^{Abc}	0.006
R4	6.67 ± 0.24^{CDEa}	5.24 ± 0.24^{Ab}	6.90 ± 0.24^{Ab}	7.38 ± 0.24^{Ab}	0.001
R5	6.90 ± 0.24^{CDEFa}	8.10 ± 0.24^{Cb}	8.10 ± 0.24^{ABCb}	9.76 ± 0.24^{Dc}	<0.001
R6	7.14 ± 0.00^{DEFa}	7.38 ± 0.24^{Bca}	7.62 ± 0.48^{ABCa}	9.52 ± 0.24^{CDb}	0.002
p-value	<0.001	<0.001	<0.001	<0.001	

Mean values followed by the same capital letter(s) within the same column do not differ significantly from one another while mean values followed by the same small letter(s) within the same row do not differ significantly from one another (α=0.05, one-way ANOVA, SNK-test).

As the free water is removed by evaporation during firing at 600°C, the contraction then depends on the particle size and the effect of the hydrogen bonds between the oxygen of the silicate and the OH of the aluminate. Again the black clay body showed the largest contraction of 10.24±0.24% followed by brown clay with 7.38±0.24% then the grey clay with 6.90±0.48%. Again curing slightly improved the packing of the clay body particles as seen from the difference in shrinkage of black cured with 10.24±0.24% as compared to black uncured with 10.48±0.24%). Increase in temperature increases the linear shrinkage

by reducing the interlayer distances through evaporation of the water from the interlayer and increased attractions between the layers.

R1 showed the lowest dry shrinkage of 5.48±0.24% but this is not significantly different from 6.19±0.24% of cured brown and 5.71% of cured grey body. This is attributed to their high sand and gravel content. The coarse sand and gravel molded in the R1 clay body reduces drastically the contraction of the clay body. It is noted that R1 with 6.67±0.24%, R2 with 7.62±0.24% and R3 with 7.14±0.41% do not differ significantly at 600°C but R4 showed a significantly smaller shrinkage of 5.24%. This shows that large size particles reduce shrinkage. The effect of contraction at varying temperatures is smaller for grey uncured body with a *p*-value 0.160 which is due to the burning out of the organic matter in the grey clay body as shown by table 4.2. As free water leaves the R4 structure during firing at 600°C, the high percentage SCBA ash increases formation of K_2SiO_3 and $CaSiO_3$ that are large size feldspars reducing shrinkage drastically (Tonnayopas, 2013). Unlike in grog all the SiO_2 in SCBA reacts as shown by the reaction equations (**10**) and (**11**) below since it is in powder form and not impeded in crystalline form.

$$K_2O_{(s)} + SiO_{2(s)} \rightarrow K_2SiO_{3(s)} \qquad \text{Equation (10)}$$

$$CaO_{(s)} + SiO_{2(s)} \rightarrow CaSiO_{3(s)} \qquad \text{Equation (11)}$$

The 5% SCBA in R5 changed the percentage particle size significantly and its reaction with silica did not yield much feldspar leading to a large shrinkage of 8.10±0.24%.

The shrinkage trends at 800°C and 1000°C are similar to that at 600°C. The black uncured clay registered the largest shrinkage of 10.71±0.00% at 800°C and 13.10±0.24% at 1000°C while uncured grey clay registered the smallest shrinkages of 7.38±0.24% and 7.38±0.24% at 800°C and 1000°C due to small paricle size in black clay.

Generally, the shrinkage of the mixtures was smaller than of pure clay bodies at all firing temperatures. This shows that even mixing of the clays improves the particle packing reducing shrinkage. Some of the shrinkage values at 1000°C agree closely with research done on Ugandan soils at 1250°C that ranged between 1.9-10.8% for six samples (Kirabira, 2003).

All the clay bodies registered higher fired shrinkage than their dry shrinkage because during firing the material sinters and densifies by forming liquid glass which increases contraction (Kirabira, 2003). Albite is solely important in this step since it offers the Na_2O required in this process according to the equations (**2**), (**12**) and (**3**) below.

$2NaAlSi_3O_{8(s)} + 3H_2O_{(l)} \rightarrow Al_2Si_2O_5(OH)_{4(s)} + 4SiO_2 + 2NaOH_{(aq)}$ Equation (**2**)

$2NaOH_{(s)} + heat \rightarrow Na_2O_{(s)} + H_2O_{(l)}$ Equation (**12**)

$Na_2O_{(s)} + SiO_{2(s)} + Heat \rightarrow Na_2SiO_{3(l)}$ (glass) Equation (**3**)

All mixture formulations showed increased contraction with increase in temperature. The contraction is smallest for R2 with a p-value of 0.33 followed by R3 at p = 0.006, R6 at p = 0.002 and R4 at p = 0.001 for the mixtures. The mixing of the clays enhances the

packing of the mineral sheets in addition to enhancing densification (Allen, 1986). Contractions in R1 and R4 at varying temperatures do not differ significantly. R6 registered a significantly high shrinkage of 9.52±0.24% at 1000°C compared to 7.62±0.48% at 800°C, 7.38±0.24% at 600°C, 7.14±0.00% at dry which means its vitrification and densification process occursat low temperatures between 800°C and 1000°C. These data are similar to those on Ugandan soils (Kirabira, 2003).

All the clays and clay mixtures showed average dry shrinkage of 5.48±0.24% to 9.76±0.24% and a fired one of 7.38±0.24% to 13.10±0.24% which fall within acceptable margin for earthenwares. Generally clays for pottery should have a dry shrinkage of 4-9% and a fired shrinkage of 7-17% (Allen, 1986).

As the free water in dickite structure leaves the interlayer distances, the negative charge on the SiO_2 and the positive charge formed on the Al^{3+}, Ca^{2+} come nearer to each other increasing the forces of attraction which contracts the sheet structure (Parashar and Parashar, 2012). Firing beyond 600°C destroys the hydrogen bonds increasing the interlayer attractions from exposed layer charges. This contracts the structure of the clay body more. For example R6 has shrinkage of 7.38±0.24% at 600°C. As temperature increases beyond 600°C bridging OH is removed as sintered material flows into the interlayer leading to even more shrinkage of 7.62±0.48% at 800°C and 9.52±0.24% at 1000°C. Rapid and large shrinkage may separate the inter layers beyond 0.72 nm in the kaolin causing cracking in the clay body (Thomas, 1998). This cracking can be enhanced by a large filler particle that develops a fault line as for the case of Ilesi potters mixture.

The larger the percentage shrinkage the higher the probability for cracking though curing reduces this cracking by between 0.2% and 0.9% as shown by table 4.17. This is due to the slow moisture absorption enabling uniform packing of the inter layers. In our case uniform packing was enhanced by sieving the dry raw materials on standard sieves that allowed the medium sand proportions to reduce effects of rapid shrinkage. The rate and quantity of shrinkage has a direct bearing on cracking of the product during drying and firing. It is also an important variable in designing the sizes of the product at forming stage i.e. it informs the potter on the dimensions of the pot at the forming stage in order to achieve the required dimensions after firing. Figure 4.15 illustrates the trend of shrinkage with temperature variation for all the clay bodies analyzed.

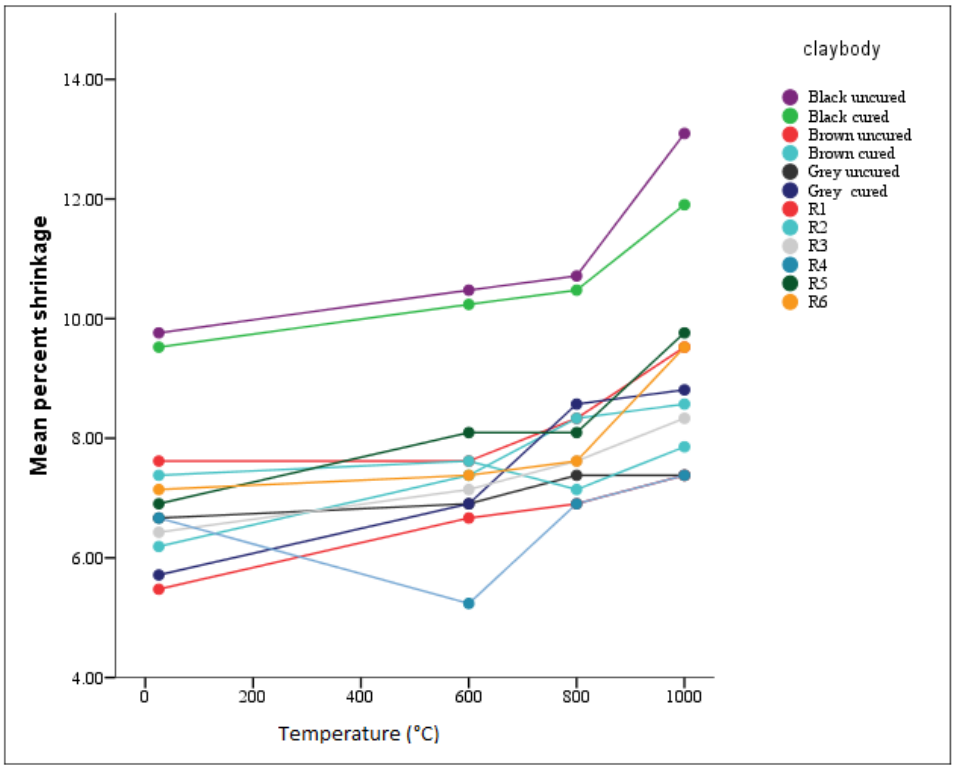

Figure 4.11: Shrinkage of dry and fired clay bodies

The line graphs for the clay bodies match a trend of increase in shrinkage with increase in firing temperature.

4.4.6 Density

The densities of molded blocks fired at various temperatures were determined in kg/m^3 using the overflow can method. The results are given in the table 4.11.

Table 4.11: Mean densities of dry and fired clay bodies

Claybody	Dry (Mean±SE) kg/m^3	600°C (Mean±SE) kg/m^3	800°C (Mean±SE) kg/m^3	1000°C (Mean±SE) kg/m^3	p-value
Black uncured	1665.26±5.55^{Ba}	1885.83±4.52^{Ed}	1732.52±6.05^{Bb}	1840.93±16.44^{Ac}	<0.001
Black cured	1873.19±4.62^{Ea}	1842.96±14.28^{Db}	1731.73±5.13^{Bb}	1817.41±29.83^{Ab}	<0.001
Brown uncured	2029.43±11.08^{H}	2049.12±10.08^{H}	1979.70±16.22^{D}	2019.76±8.59^{B}	0.018
Brown cured	1930.91±4.37^{Fa}	2016.75±9.93^{GHb}	1961.60±11.86^{Da}	2148.68±25.59^{Cc}	<0.001
Grey uncured	1976.61±8.58^{G}	1994.22±22.36^{G}	1976.35±15.54^{D}	2014.25±5.11^{B}	0.278
Greycured	1967.31±22.02^{G}	1961.25±13.94^{F}	1996.03±28.19^{D}	2008.86±2.95^{B}	0.312
R1	2359.98±26.68^{Jc}	2017.87±0.35^{Gha}	2056.15±6.67^{Ea}	2138.62±11.36^{Cb}	<0.001
R2	2048.02±11.49^{Hb}	2056.53±17.37^{Hb}	1877.00±13.37^{Ca}	2338.83±1.57^{Dc}	<0.001
R3	2213.93±5.97^{Ic}	1892.13±3.38^{Ea}	1883.69±8.43^{Ca}	2019.86±20.92^{Bb}	<0.001
R4	1572.06±6.70^{Aa}	1576.74±7.37^{Aa}	1567.39±17.14^{Aa}	1816.99±12.13^{Ab}	<0.001
R5	1741.34±10.87^{Ca}	1753.08±3.05^{Bab}	1771.92±5.83^{Bb}	1842.99±6.50^{Ac}	<0.001
R6	1823.51±5.11^{Db}	1805.71±2.87^{Ca}	1858.54±6.05^{Cc}	2023.50±3.47^{Bd}	<0.001
P-value	<0.001	<0.001	<0.001	<0.001	

Mean values followed by the same capital letter(s) within the same column do not differ significantly from one another while mean values followed by the same small letter(s) within the same row do not differ significantly from one another (α=0.05, one-way ANOVA, SNK-test).

The densities of different clay bodies were significantly different. The black clay body showed the lowest density while the brown showed the highest. This trend is generally replecated at 600°C, 800°C and 1000°C. Finer textures like in black as shown by table 4.2 have higher compaction which leads to lower densities due to the small size particles that contribute less to the mass of the clay body. The brown and grey clays have higher percentage sand at 64% and 52% respectively as per table 4.7 hence higher mass value

factor which explains why they have higher densities than the black. Table 4.11 shows that the densities for the cured clay bodies are generally lower than for uncured a trend that is seen for clay bodies at 600°C, 800°C and 1000°C. Curing closes the pores with water molecules expanding the volume occupied by the clay body reducing the density.

Among the clay mixtures, R4 registered the lowest density of 1572.06±6.70 kg/m^{3}after R5 with 1741.34±10.87kg/m^3. This maybe attributed to the effect of SCBA which is very fine and contributes very little to the mass of the clay body (Tonnayopas, 2013). R1 has the highest density of 2359.98±26.68 kg/m^3. This is due to the large percentage of the gravel and sand in the clays. R3 with a 30% grog sand has higher value 2359.98±26.68 kg/m^3 than R2 at 2048.02±11.49 kg/m^3 whose grog sand percentage is 20%. R6 registereda modest density of 1823.51±5.11 kg/m^3 due to its lower grog sand content. The density trends for the clay bodies at 600°C, and 800°C are similar to those of the dry bodies. For example, at 600°C R2 has the largest density of 2056.53±17.37 kg/m^3 followed by R1, 2017.87±0.35 kg/m^3. R4 and R5 again registered the lowest values. At these temperatures all the free water has evaporated out and the densities then wholly depend on the packing of the particles and the effects of the interlayer forces.

The values of density of these clay bodies fall within ranges of other clay bodies like at Abakalika in Nigeria(Nweke, 2007), in Uganda(Kirabira, 2003).Figure 4.12 shows the variations in mean densities of fired clay bodies.

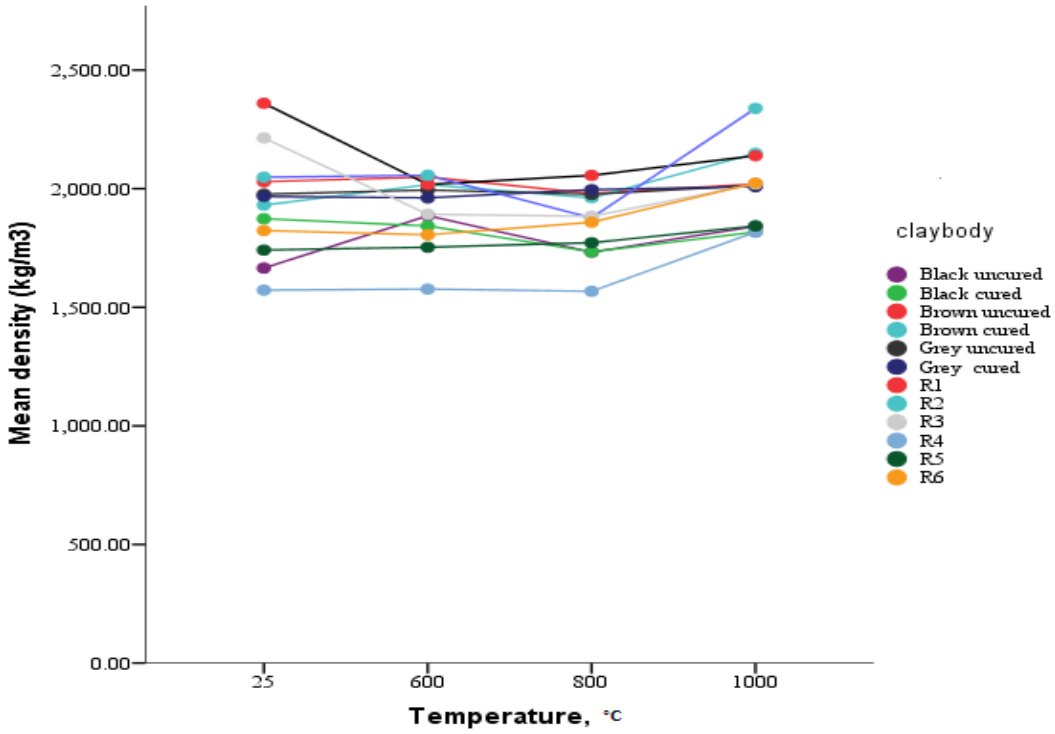

Figure 4.12: Densities of dry and fired clay bodies

The densities of dry bodies were significantly different from those of the fired clay bodies except for the brown uncured, grey cured and grey uncured. There was gradual increase in the densities of the clay bodies with increase in temperature. The density of the black uncured body increases from 1665.26±5.55 kg/m^3 at dry to 1885.83±4.52 kg/m^3 at 600°C. The evaporation of the free water reduces the clay body's volume and leads to stronger inter-layer attractions from the hydrogen bonds and accessory ions which reduce the volume occupied thereby increasing the density. The density of clay bodies reduces at 800°C as the body loses the bound water changing the crystal phase due to vitrification. For example, black uncured reduced to 1732.52±6.05 kg/m^3 from 1885.83±4.52 kg/m^3 at 600°C. The crystal phase begins to change again from 1000°C as the liquid glass formed

fills the pores. The sheets become exposed directly to the interlayer attractions which make the structure more rigid. This increases the density as seen in the black uncured from 1732.52±6.05 kg/m^3 to 1840.93±16.44 kg/m^3 as this reduces the volume of the clay body.

4.4.7 Porosity of fired clay bodies

Porosity in soils represents the voids or empty spaces between the soil particles or aggregates. The pore size distribution, clay particle size, distribution of clays within the pore space and the composition of clays are important factors in controlling porosity or permeability relationships. Table 4.12 gives the values of porosity of fired clay bodies.

Table 4.12: Porosities of fired clay bodies

	%Mean porosity ±SE			
Claybody	600°C	800°C	1000°C	p-value
Black uncured	17.80±0.02^{Aba}	25.70±0.30^{Eb}	24.80±0.46^{Db}	<0.001
Black cured	17.79±0.14^{Aba}	20.09±0.06^{Db}	17.97±0.09^{Aba}	<0.001
Brown uncured	15.96±0.74^{ABC}	17.53±0.23^{B}	17.79±0.16^{AB}	0.060
Brown cured	14.16±0.09^{Aa}	16.02±0.12^{Ab}	16.37±0.16^{Ab}	<0.001
Grey uncured	15.73±0.65^{Aba}	18.09±0.25^{Abb}	16.91±0.11^{Aab}	0.018
Grey cured	15.36±0.03^{Aba}	17.04±0.20^{Bb}	16.81±0.10^{Ab}	<0.001
R1	17.08±0.11^{Bca}	18.14±0.08^{Abb}	17.89±0.14^{Abb}	0.002
R2	16.60±0.18^{Bca}	19.29±0.71^{CDb}	17.90±0.21^{Abab}	0.014
R3	16.71±0.14^{Bca}	18.24±0.14^{Abc}	17.57±0.22^{Abb}	0.002
R4	32.65±0.55^{Fa}	35.12±0.35^{Fb}	31.18±0.83^{Ea}	0.010
R5	20.10±0.96^{D}	19.42±0.20^{CD}	20.53±0.39^{BC}	0.472
R6	22.17±0.31^{E}	19.26±0.49^{CD}	19.61±1.27^{BC}	0.083
p-value	<0.001	<0.001	<0.001	

Mean values followed by the same capital letter(s) within the same column do not differ significantly from one another while mean values followed by the same small letter(s) within the same row do not differ significantly from one another (α=0.05, one-way ANOVA, SNK-test).

At 600°C, the porosities of the black, brown and grey clay bodies are not significantly different though these clay bodies have lower porosities than the recipes. This is expected since they all have the same clay minerals as seen from table 4.2. At 600°C, all the free water is evaporated from the clay body but the pore throats are not expanded hence lower percentage moisture uptake (Olubayode *et al.*, 2015).

Cured clay bodies have lower porosities than the uncured clay bodies. Brown uncured had 15.96±0.74% while brown cured posted 14.16±0.09% at 600°C. Curing therefore increases density packing which closes some of the pores.

At 800°C, the same trend as at 600°C is observed. Cured clay bodies have lower porosity than uncured. For instance black cured had a porosity of 20.09±0.06% while uncured was 25.70±0.30%. Curing as earlier discussed improves the packing of the particles during the moulding, which locks out most of the pores from the pore throats. The porosities of fired bodies at 800°Care higher than those at 600°C. For example, black cured had 17.79±0.14% at 600°C while at 800°C was 20.09±0.06%. This is because at 800°C the clay bodies expand due to increased kinetic energy, opening the pores more which facilitates the absorption of water (Nweke, 2007).

At 1000°C the porosity values are lower than at 800°C which points at the possibility of these clays vitrifying at slightly lower temperatures than 1000°C. The formed liquid glass flows into the pores and blocks them reducing porosity (Abolarin *et al*., 2006). This

property makes these clays very suitable for pottery since they will fire at low maturing temperatures.

The porosities determined for R1, R2 and R3 are not significantly different. R4 had the highest value of 32.65±0.55% because most of its moisture R4 was absorbed by the SCBA. SCBA has comparatively higher percentages of P_2O_5, K_2O and CaO which absorb the moisture (Olubayode *et al.,* 2015) according to the following equations:

$$P_2O_{5(s)} + H_2O_{(l)} \rightarrow H_3PO_{4(aq)} \qquad \text{Equation (}\mathbf{13}\text{)}$$

$$K_2O_{(s)} + H_2O_{(l)} \rightarrow 2KOH_{(aq)} \qquad \text{Equation (}\mathbf{14}\text{)}$$

$$CaO_{(s)} + H_2O_{(l)} \rightarrow Ca(OH)_{2(aq)} \qquad \text{Equation (}\mathbf{15}\text{)}$$

R4 and R5 have higher values of 35.12±0.35% and 19.42±0.20% respectively, among the mixtures attributed to the effect of the SCBA. These values compare well with clay bodies elsewhere like research on soils in Uganda (Kirabira, 2003).

With exceptions of R5 and R6, the rest of the clay bodies showed that the grog sand and quartz sintered the clay body at temperatures of between 800°C and 1000°C. The value of R5 from 20.53±0.39% to19.42±0.20% and R6, 22.17±0.31^{E} to 19.26±0.49% showed that these clay mixtures sintered at lower temperatures of between 600°C and 800°C which make them most suited for pottery. The data is similar to the densities and porosity research at Abaliki in Nigeria (Nweke, 2007).

Water entering the interlayer results in ion or particle movements, which results into dynamic permeability reduction caused by clay particles moving and becoming trapped at

subcritical pore throats (Morris and Shepperd, 1992). This reduction observed at 1000°C on figure 4.18 is due to the adsorption of clay particles within the pore space which shows an increase in porosity up to 800°C followed by a reduction at 1000°C. Figure 4.18 gives the relationship between porosity and temperatures.

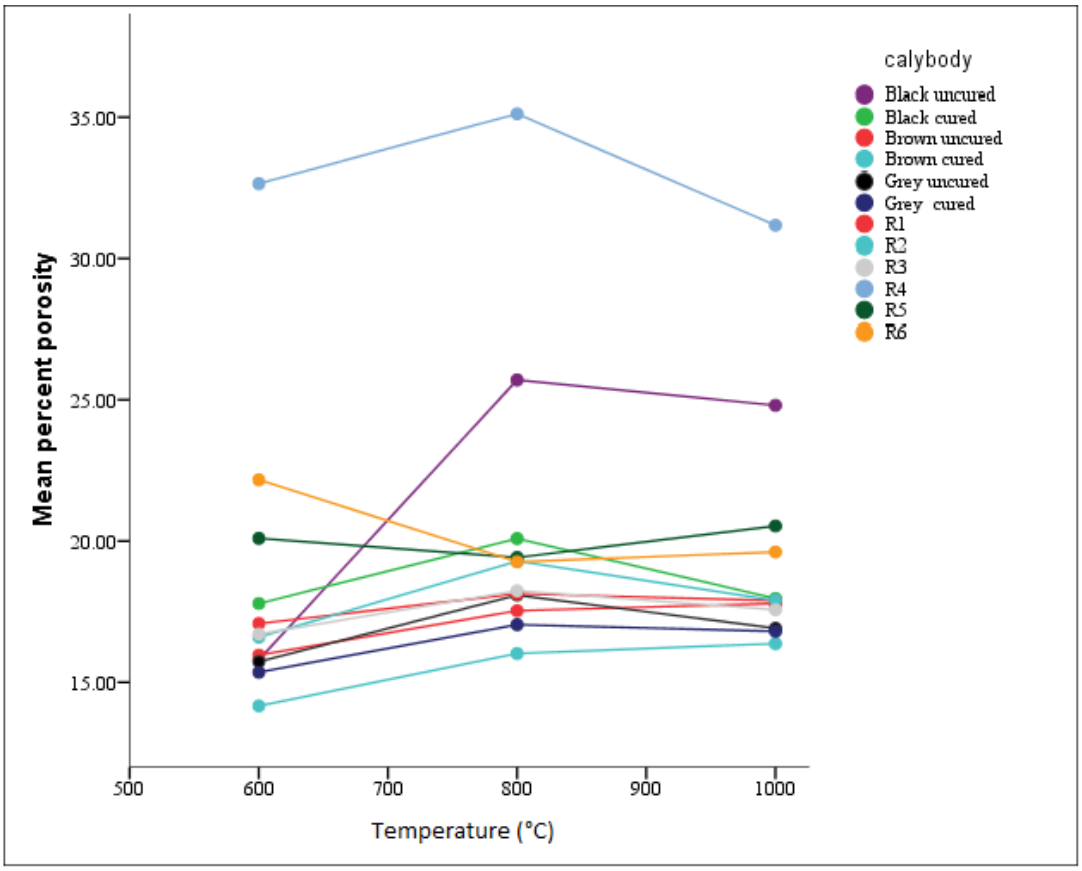

Figure 4.13: Porosity of fired clay bodies

The general increase in porosity between 600°C and 800°C as seen in figure 4.13 is due to the expansions of the clay body that open and increases the pore holes but as the body begins to sinter at about 1000°C, the pore throats begin to close and greater movement of the dickite aggregates blocks these pore throats reducing porosity. This is different for the trend in R5 and R6 which reduces at 800°C. This would mean these mixtures offer

uniform particle packing that lowers the vitrification temperature a property that would reduce on fuel consumption during kilning. Small expansions of clay are sufficient to block or partly block the small pore throats as a result of increase in temperatures of the clay body (Nimmo, 2004). The small pore throats are also blocked by the physical movement of the dickite particles that occur as free aggregates.

4.4.8 Compressive strength

Compressive strength refers to the amount of force required to fail or rupture the clay body structure. The compressive strength of dried and baked blocks was determined using universal crushing machine and the rupture values are given in table 4.21.

Table 4.13: Compressive strengths of green and fired clay bodies

	Mean compressive strength ±SE/Mpa				
Clay body	**Green**	**600°C**	**800°C**	**1000°C**	**p-values**
Black uncured	22.17 ± 1.12^{Aa}	32.71 ± 0.93^{Bb}	35.12 ± 0.59^{Abb}	37.03 ± 1.54^{Ab}	<0.001
Black cured	23.04 ± 0.68^{Aba}	32.74 ± 0.62^{Bb}	36.37 ± 0.26^{Abc}	43.55 ± 1.76^{Abd}	<0.001
Brown uncured	24.50 ± 0.51^{BCDa}	31.03 ± 0.17^{Bb}	36.20 ± 0.68^{Abb}	49.21 ± 3.86^{Bc}	<0.001
Brown cured	26.22 ± 0.34^{Dea}	32.66 ± 0.91^{Bb}	37.25 ± 0.03^{Abb}	45.05 ± 2.81^{Abc}	<0.001
Grey uncured	22.67 ± 0.30^{Aba}	31.53 ± 0.73^{Bb}	34.10 ± 0.25^{Ab}	42.10 ± 2.68^{Abc}	<0.001
Grey cured	24.40 ± 0.25^{BCDa}	32.36 ± 1.65^{Bb}	36.40 ± 0.25^{Abc}	41.91 ± 1.26^{Abd}	<0.001
R1	23.30 ± 0.21^{Aba}	24.92 ± 0.37^{Aa}	33.29 ± 2.37^{Ab}	37.27 ± 1.54^{Ab}	<0.001
R2	23.83 ± 0.42^{ABCa}	26.37 ± 0.65^{Aa}	39.70 ± 1.10^{Bb}	44.10 ± 2.19^{Abc}	<0.001
R3	25.58 ± 0.14^{CDEa}	31.47 ± 0.73^{Bb}	38.34 ± 0.09^{Abc}	48.57 ± 1.71^{Bd}	<0.001
R4	24.88 ± 0.49^{BCDEa}	30.76 ± 0.63^{Bb}	35.87 ± 0.54^{Abc}	37.98 ± 0.41^{Ad}	<0.001
R5	26.67 ± 0.32^{Ea}	33.03 ± 0.19^{Bb}	39.90 ± 0.38^{Bc}	43.86 ± 0.53^{Abd}	<0.001
R6	28.83 ± 0.20^{Fa}	39.18 ± 1.52^{Cb}	44.37 ± 2.23^{Cc}	49.23 ± 1.35^{Bc}	<0.001
P-value	<0.001	<0.001	<0.001	0.001	

Mean values followed by the same capital letter(s) within the same column do not differ significantly from one another while mean values followed by the same small letter(s) within the same row do not differ significantly from one another (α=0.05, one-way ANOVA, SNK-test).

The cured brown clay blocks posted highest value of green compressive strengthof 26.22±0.34 MPa followed by cured grey 24.40±0.25 MPa while the blocks of cured black had the lowest 23.04±0.68 MPa. This can be attributed to the uniform packing of the particles in the brown and grey. The black clay is composed of very fine clay and silt particles with few sand particles that make the packing uneven.

The data also shows that curing improves compressive strengths by improving the packing of the particles at the molding stage such that when the water leaves the body, it leaves many contact points. For example, the green compressive strength of black cured was 23.04±0.68 MPa while that for the uncuredwas 22.17±1.12 MPa. This trend is seen within the values at 600°C and 800°C.

The green compressive strength is attributed to the hydrogen bonds between the oxygen of the silicate tetrahedral sheets and the OH of the octahedral sheets. As free water filters out of the body, the interlayers get closer increasing the contact points and effects of hydrogen and Van der Waals forces (Olubayode *et al.,* 2015). Trend of green compressive strengths is similar to those at 600°C and 800°C. These values are close to those determined in Nigeria clays at 800°C (Nweke, 2008).

Increasing temperature to 600°C and 800°C sinters the clay body increasing the effects of attraction forces in the clay unit structure (Twubahimana, and Mbereyaho, 2013). There is therefore, a general increase in values as temperature of clay bodies is increased from 600°C to 1000°C. For example, the black cured value increased from 32.74±0.62 MPa at

600°C through 36.37±0.26 Mpa at 800°C to 43.55±1.76 MPa at 1000°C. This data is similar to research done on clays in Uganda (Kirabira, 2003).

Clay blocks made from R6 clay mixture had significantly higher compressive strength than the other mixtures with R1 posting the lowest value of 23.30±0.21 MPa. This can be attributed to both curing and more uniform packing of the clay particles in R6. R4 had compressive strength of 24.88±0.49 MPa which is within the KEBS standards of 7-27 MPa for clay bricks.This strength arises from the glassing reaction between the powder silica in SCBA and the albite (Tonnayopas, 2013).These values are similar to the ones observed for the Nweke blends (Nweke, 2007).

As the water in the interlayer is expelled, the charges across the layers become enhanced causing a more rigid structure. However, these forces are destroyed beyond 900°C, causing intercalation of the glass phase reducing the internal lattice. It is however apparent from the data that sintering and densification occurs up to 1000°C which is enhanced by glass formation. Figure 4.19 shows the relationship between compressive strengths and temperature.

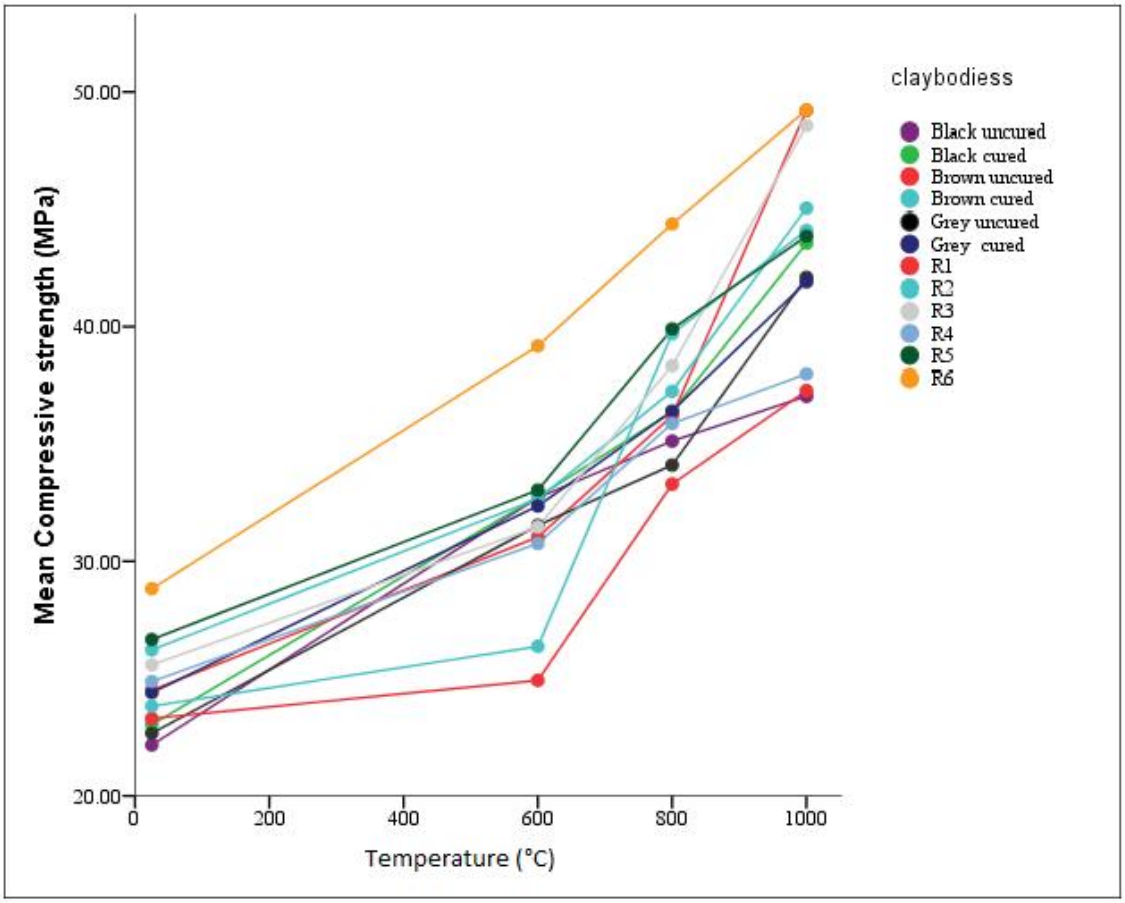

Figure 4.14: Compressive strength of dry and fired clay bodies

There is uniform increase in the compressive strengths with increase in firing temperature of the clay bodies. The trend for R6 was uniform implying that the ratio develops uniform packing for the particles. The R3 and R6 values fall within KEBS standards, a minimum of 48.5 MPa for engineering bricks.

When water is removed from a clay body by drying, the particles come closer to each other hence short distance Van der Waal's forces will be operating at these points of contact and these may be supplemented by the binding effect of any soluble matter left

behind when the water evaporated. As the packing improves, by removal of the interlayer water and ions, the number of points of contact rapidly increases (Allen, 1986). Reducing the particle size and improving on packing drastically increases the unfired strength which was achieved by milling and sieving the clays and sand on standard sieves.

4.4.9 Losses

Table 4.14 shows Losses that were incurred during the research using the shrinkage parameter. The data shows that R6 is a superior clay mixture to the others.

Table 4.14: Losses incurred using shrinkage tests

Clay body	No. of pieces	Swelling /molding	% Loss in time	Cracking /drying	Cracking /firing	% Losses
Blackuncured	12	2	17	0	0	0
Blackcured	12	1	8	0	0	0
Brown Uncured	12	0	0	1	1	17
Brown Cured	12	0	0	0	0	0
Grey uncured	12	1	8	0	0	8
Grey cured	12	0	0	0	0	0
R1	12	4	33	2	1	25
R2	12	0	0	1	0	8
R3	12	0	0	1	0	8
R4	12	2	8	1	1	18
R5	12	1	17	0	0	0
R6	12	0	0	0	0	0

The black clay body showed loss in time of 17% due to swelling. The black clay is very fine and sticky due to high percent clay and silt of 62% as illustrated by table 4.7. Molding of black uncured will have a lot of swelling particularly if the soil is not sufficiently plastic which is responsible for the high percent loss in time of 17%. This argument is supported by the 8% for the black cured. Stabilization of the mold due to curing is responsible for the reduction in the losses from 17% to 8%. Brown uncured had the highest percent losses of 17% occasioned by the sand particles of 64% shown in table 4.7 in its mold. This argument is supported by the value of grey uncured of 8% with a

sand fraction of 52% from the same table 4.7. Whereas formation of clay mixtures improves workability and a number of other physical properties, it however increases losses if the ratios are not right. R1 is easy to work with but had higher swelling of 33% and breakages of 25%. This is due to the large coarse sand and gravel particles that cause fault lines during drying which is enhanced during firing causing the cracking and on spot breaking.

R4 had a relatively high percent swelling of 8% and percent cracking of 18%. This is explained by the large proportion of solid ash. This solid ash traps water at the sites causing swelling and on drying leaves large voids that act as fault lines for cracking. R2 and R3 have 20% and 30% grog sand respectively. This grog sand that acts as filler will equally develop fault line centers as water evaporates out hence recording losses of 8%. R6 with 25% black and 15% grog sand appear to have formed a mixture with uniform particle sizes hence easy workability and zero percent losses. The physical properties shown in table 4.15 were used to compare the suitability of the formed mixtures.

Table 4.15: Physical parameters at 800°C

Clay body	**Density/ Kg/M^3 (Mean±SE)**	**% shrinkage (Mean±SE)**	**%Moisture (Mean±SE)**	**Strength (Mean±SE)MPa**	**Porosity (Mean±SE)**
R1	2056.15±6.67^{Ea}	6.90±0.24^{Ab}	26.00±0.19^{ab}	33.29±2.37^{Ab}	18.14±0.08^{Abb}
R2	1877.00±13.37^{Ca}	7.14±0.41^{AB}	28.91±0.10^{bc}	39.70±1.10^{Bb}	19.29±0.71^{CDb}
R3	1883.69±8.43^{Ca}	7.62±0.24^{ABCbc}	27.82±0.05^{abc}	38.34±0.09^{Abc}	18.24±0.14^{Abc}
R4	1567.39±17.14^{Aa}	6.90±0.24^{Ab}	42.35±0.11^{e}	35.87±0.54^{Abc}	35.12±0.35^{Fb}
R5	1771.92±5.83^{Bb}	8.10±0.24^{ABCb}	36.06±0.56^{d}	39.90±0.38^{Bc}	19.42±0.20^{CD}
R6	1858.54±6.05^{Cc}	7.62±0.48^{ABCa}	30.53±2.75^{c}	44.37±2.23^{Cc}	19.26±0.49^{CD}
P-value	<0.001	<0.001	<0.001	<0.001	<0.001

Key: red indicates best parameters, blue indicates most suiting parameters

The ratios used in R6, R3 and R2 as shown in table 4.15 resulted in uniform packing that resulted into generally superior physical properties. The SCBA in R4 and R5 reduced their densities giving the products advantage of lightness. The SiO_2 in SCBA is wholly used in glass formation and not as filler which enables the densification and vitrification processes in R4 and R5 to occur at lower firing temperatures (Tonnayopas, 2003).

Both R6 and R3 post equal most suiting parameters as seen in table 4.15. R3 registered most suiting results on density of 1883.69±8.43 kg/m^3, shrinkage of 7.62±0.24^A% and porosity of 18.24±0.14%. Such a clay body will produce durable table and kitchen wares. R6 had most suiting ones of shrinkage 7.62±0.48%, moisture, 30.53±2.75%, a vitrification at between 600°C-800°C and compressive strength of 44.37±2.23 Mpa which will be most suitable for refractories, tiles and decorative ornaments. However R6 has 0% Lossess while R3 has 8% Lossess. This makes R6 the best choice for pottery from the Ilesi clays.

CHAPTER FIVE

CONCLUSIONS AND RECOMMENDATIONS

5.1 Conclusions

Ilesi clays were sampled and characterized. FTIR and XRD spectroscopy have revealed that the clays contain the clay minerals necessary for pottery namely, dickite, 6-16%, albite and microcline, 16-45% and quartz, 24-35%. The EDX results showed that the clays have high SiO_2:Al_2O_3 ratio of 3:1 which is suitable for pottery.

The value of physical parameters determined for the clays fall within the ranges required for clays suitable for pottery. These are, a dry linear shrinkage of 5.71-9.52%, a fired linear shrinkage of 6.9-13.1%, Porosity of 14.16-24.8%, density between 1665.26-2148.68 kg/m^3, green compressive strength of 22.17-26.22 MPa and fired compressive strength of 31.03-49.21 MPa and that curing drastically reduces losses.

The study also found out that there is no loss incurred when clay for pottery was mixed as follows, 25% black clay, 30% brown clay, 30% grey clay and 15% grog sand and then cured for 21 days.

5.2 Recommendations

It is recommended that the potters mix the clays in the proper ratios before use. The potters should process their clays by dry beneficiation, sieve and cure their clay bodies to reduce the losses during molding, drying and firing.

5.3 Recommendation for further work.

Considering that the potters remove their clay from a one acre river valley, exploration need to be undertaken to identify other deposit sites that can sustain large scale pottery industry. More studies should be conducted on the possibility of utilizing sugarcane baggase in pottery.

REFERENCES

Abolarin, M. S., Olugboji, O. A. and Ogwuoke, I. C. (2006), Determination of moulding properties of locally available Clays for casting operations, *University Journal of Technology, Thailand,* **9**(4): 238-241.

Abuh, M. A, Abia-Bassey, N, Udeinya, T. C, Nwannewuihe, H. U, Abong, A. A and Akpomie, K. G. (2014), Industrial Potentials of Adiabo Clay in Calabar Municipality of Cross River State. *The pacific Journal of Science and Technology*, **15**(1):63-74.

Adelabu, S. O. (2012), Documentation, Application and Utilization of Clay minerals in Kaduna state Nigeria, Creative Commons attribution Licence, http//dx.doi.org/10.5772/48093 pp 1-18.

Agbalajobi, S. A. and Omoijuanfo, I. S. (2012), Investigating the Strength and Porosity characteristics of some fired Clays in EDO and DELTA states. *Journal on Engineering and Applied Sciences,* **4**: 9-15.

Allen, D. (1986). Pottery Science, Materials, Processes and Products: Ellis Horwood Publishers Ltd, Chichester UK pp 21-37.

Amadala, B. (2013). Pottery transforming lives in Kakamega, *www.businessdailyafrica.com*, posted on 29.4.2013.

Amponsah-Dacosta, F., Muzerengi. C., Mhlongo, S. E and Mukwevho, G. (2013), Characterization of Clays for making Ceramic pots and Water filters at Makondeni, Limpopo province, South Africa. *ARPN Journal of Engineering and Applied Sciences,* **8:**11.

Bain, J.A. (1971), A Plasticity chart as an aid to Identification and Assessment of Industrial clays, *Journal of Clay Mineral,* **9:**1-17.

Barsom, M. W. (2003). Fundamentals of Ceramics, Drexel Univ. USA, Taylor and Francis Group Publishers New York pp 354-356.

Bohn, H. L, McNeal, B. L and O'Connor, G. A. (2001), Soil Chemistry, John Wiley and sons, 3rdEdition pp129- 143.

Bonitsky, D. and Hammer, N. M. (1986), Experiments in ceramics technology: the effects of various tempering materials on impact and thermal shock resistance. *American Antiquity,* **51**: 89-101.

Bordeepong, S., Bhongsuwan, D., Thongchai, P and Bhongsuwan, T. (2012), Mineralogy, chemical composition and ceramics properties of clay deposits in southern Thailand, *Kasetsart Journal. Natural Sciences,* **46**:485-500.

Christine, M. D. (2013), Methods for Determination of Heavy Metals and Metalloids in soils, Univ. of Strathclyde.295, Glasgow, Scotland, UK **22:** 97-121.

Dean Jr, W. E. (1974), Determination of carbonate and organic matter in calcareous sediments and sedimentary rocks by loss on ignition: comparison with other methods. *Journal of Sedimentary Research,* **44**(1): 242-248.

Ding, Z., Klopogge, J. T and Frost, R. L. (2001). Porous Clays and Pillared Clays-Based Catalysts part 2: A Review of the Catalytic and Molecular Sieve Applications. *Journal on Porous Materials,* **8:**273-293.

Edward, H. K., Walter, F. H and Lewis, S. R. (1976), Mineralogy, an Introduction to study of minerals and crystals, Krypton New Jersey pp 40-41.

Feng, T. W. (2000), Fall- cone penetration and water content relationships of clays. *Geotechnique.* **50**(2): 181-187.

Folorunso, D. O., Olubambi, P and Borode, J. O. (2014), Characterization and qualitative Analysis of some Nigerian clay deposits for refractory applications, *IOSR Journal of Applied Chemistry,* **7**: 40-47.

Garrison, S. (1989), The Chemistry of Soils, Oxford Univ. Press, Inc. New York pp 128-143.

Ghildyal, P. B and Tripathi, R. P. (1986), Soil Physics, New Age International (P) limited Publishers. New Delhi. India pp 84-85.

Gieseking, E. L. (1975), Soil Components Vol.2. Spinger-Verlag, New York. Inc. pp 98-100.

Glenn, C. N and Burkett, R. (2002), Ceramics: A Potters Handbook, 6th Edition, Wadsworth Thompson Learning, USA pp 103-105.

Goldin, A. (1987), Reassessing the use of loss on ignition for estimating organic matter content in noncalcareous soils, *Communications in Soil Science & Plant Analysis,* **18**(10): 1111-1116.

Gosselain, O. P. (1992), The bonfire of inquiries, Pottery firing temperature in archaeology: what for? *Journal of Archaeological Science*, **19**: 243-259.

Gosselain, O. P. (2000), Materializing Identities: an African perspective, *Journal of Archeological Method and Theory*,**7**: 187-217

Greenland, D. J and Hayes, M. B. (1991), The Chemistry of Soil Processes, John Wiley and sons, Toronto pp 4-5.

Grim, R. E. (1962), Applied Clay Mineralogy, McGraw-Hill Book Co., Inc., New York **136** pp 870-871.

Grimshaw, R. W. (1971), The chemistry and Physics of clays and allied ceramic materials, New York, 4TH Edition pp 272-290.

Gussenheim, S and Martin, R. T. (1995), Definition of clay and clay mineral: Joint Report of the AIPEA nomenclature and CMS nomenclature committees; *a Journal of Clays and Clay Minerals.* **44**:713-715.

Heckroodt, R. O. (1991), Clays and Clay minerals in South Africa, *Journal of South African Institute of Mineral Metallurgy,* **91:** 341-345.

Heimann, R and Franklin, U.M. (1979), Archaeothermometry, the assessment of firing temperatures of ancient ceramics, *Journal of the International Institute of Conservation-Canadian Group,* **4**:23-45.

Hesse, P. R. (1971), A Text book of Soil Chemical Analysis, Chemical Publishing, New York pp 120-467.

James,O. O., Adediran, M., Adekola, E. O., Odebunmi, E. O and Adekeye, J. I. D. (2008), Beneficiation and characterization of a bentonite from North Eastern Nigeria. *Journal of the North Carolina Academy of Science,* **124**(4): 154-158.

Jana, M and Peter, K. (2001), Baseline studies of clay minerals society, Source of clays: Infrared methods. *Clay and Clay Minerals,* **49**:410-432.

Jovanovic, M. and Mujkanovic, A., (2013), Characterization, beneficiation and utilization of clay from central Bosnia, B&H. 17th International research/export conference pp 1-4.

Juan, I.S., Rosa M., Enrique, L., Christino, J. D., Blanca, M, R, Z., Jose, M. G., Silvino, C and Pedro, E.M. (2004), Loss on ignition: a qualitative or quantitative method for organic matter and carbonate content in sediments pp 1-2.

Karoki, B. K. (2008), Analysis and treatment of clays to assess their value as source of aluminium and ceramics products, MSc thesis. Kenyatta University pp 2-81.

Katherine, O and Benjamin, F. K. (1996), X-ray diffraction analysis of thin clay films from dilute suspensions using glancing incidence diffraction. *Clays and Clay Minerals* **44**:811-817.

Kent, D. F. (2008), Zulu Pottery in the Lower Thukela Basin, KwaZulu- Natal, South Africa, *Southern African Humanities,* **20**: 477-511.

Kirabira, J. B. (2003), Characterization of Uganda raw materials for bricks before and after sintering, Licentiate thesis, Royal Institute of Technology pp 1- 16.

Kirk, R. E. and Othmer, D. E. (2004), Encyclopedia of Chemical Technology, 5th Edition, John Wiley& sons, New York **6**: 658-701.

Klinefelter, T. A. and Hamlin, H. P. (1957), Syllabus of clay Testing. Bureau of Mines, USA, Bulletin 0565 pp 30-40.

Lee, J. D. (1986), Concise Inorganic Chemistry, 5th-Edition pp 440-444.

Lenka, V and Eva P. (2005), Identification of clay minerals and micas in sedimentary rocks, *Acta Geodyn. Geomater*, **2**: 167-175

Maggate, M., Neururer, Ch and Ramseyer, D. (2010), Temperature evolution inside a pot during experimental surface (bornfire) firing, *Applied Clay Science.* **53**(3): 500-508.

Mugagga, F., Kagembo, V and Buyinza, M. (2010), A characterization of the physical properties of soil and implications for landslide occurrence of the slopes of Mount Elgon Eastern Uganda, *Journal of International Society for the Prevention and Mitigation of Natural Hazards*, **52**(1):12-14.

Mohsen. Q. and El-maghraby, A. (2010), Characterization and Assessment of Saudi Arabia clays, Raw materials at different areas, *Arabian Journal of Chemistry*, **3**: 271-277.

Morris. K. A and Shepperd. C. M. (1992), Characteristics in the Bridport Sands of Wytch Farm, Dorset, *Clay Minerals*, **17:**41-54.

Mukherjee, S. and Ghosh, B. K (2013), The Science of Clays, Applications in Industry, Engineering and Environment, Capital publishing company, India pp 5-11.

Murray, H. D. (2002), Industrial Clays: Case study, International Institute for environment and Development, (IIED), England, pp 1-4.

Nweke, E. S. and Ugwu, E. I. (2007), Analysis and characterization of clay soil in Abakaliki, *The Pacific Journal of Science and Technology*, *Nigeria* **8**:190-193.

Nimmo, J. R. (2004), Porosity and Pore Size distribution, Encyclopedia of Soils in the environment, pp 295-303.

Nwosu, D. C., Ejikeme, P. C. N and Ejikeme, E. M. (2013), Physic-Chemical Characterization of NGWO white Clay for industrial use. *International Journal of Multidisciplinary Sciences and Engineering*, **4** (3): 1-4.

Olale, A. E. (1985), Silicate Technology. Kenya Literature Bureau, Nairobi pp3-4.

Olubayode, S. A., Olateju, O. T., Awokola, O.S., Dare, E. O., Akinwamide, J. T., and Eshiett, L.M. (2015), Engineering properties of saw dust Modified clay soil. *International Journal of Pure and Applied Bioscience.* **3**(5):35-41.

Osabar, V. N., Okafor, P. C., Ibe, K. A and Ayi, A. A. (2009), Characterization of clays in Udukpani, South eastern Nigeria. *African Journal of Pure and Applied Chemistry*, **3**:79-85.

Parashar, K. A and Parashar, R. (2012), Comparative study of Compressive Strengths of bricks made with various materials to clay bricks. *International Journal of Scientific and Research,* **2**:1-4.

Preeti, S. N and Singh, B. K. (2007), Instrumental characterization of clays by XRF, XRD and FTIR, *Bull. Materials Science,* **30**(3):1-4.

Ronald, J. G. (1967), Quantitative x-ray diffraction analysis using clay mineral standards extracted from the samples to be analyzed, *Clay Minerals,* **7**:79.

Rogers, D. (2006), Subsurface Exploration Using the Standard Penetration Test and the Cone Penetration Test, Environmental and Engineering, *Geoscience,* **11**:61-179.

Rusovich-Yugai, N. S. and Neklyudova, T. L.(2007), Color Characteristics of Low Melting Clays. *Clay Minerals,* **64:**232-234.

Skibo, J. M., Schiffer, M. B. and Reid, K. C. (1989), Organic tempered pottery; an experimental study, *American Antiquity,* **54**: 122- 146.

Sposito, G.N. (1989), The Chemistry of Soils. Oxford University Press, London pp 29-31.

Stone, K. J. L. and Phan, K. D. (1995), Cone penetration test near the plastic limit. *Geotechnique,* **45**(1): 155-158.

Tan, K. H. (2011), Principles of Soil Chemistry, 4th Edition, CRC press pp160-169.

Teixeira S. R., De Souza S. A and Moura, C. A. I. (2001), Mineralogical characterization of clays used in the structural ceramic industry in west of S. Paulo State, Brazil. *Ceramica,* **47**(304):204-206

Tite, M. S. (2008), Ceramics production, Provenance and Use- A Review- Research Laboratory of Archeology and the history of Art, Dyson Perrins Building, South Parks road, Oxford OX 1 3QY UK. *Journal on Archaeometry*. **50**:216-231.

Thomas, P. J. (1998), Quantifying properties and variability of expansive soils in selectedmap units, Doctoral dissertation, Virginia Polytechnic Institute and State University) pp 15-89.

Thompson D. (1995), Insights into Specialty, Inorganic Chemicals, The Royal Society of Chemistry pp 330-333.

Tonnayopas, D. (2013), Green Building Bricks Made with Clays and Sugar Cane Baggase Ash. *Materials, Science and Technology*, **18**: 7-12.

Twubahimana, J. D and Mbereyaho, L. (2013), Impact of clay particles on concrete Compressive Strength, *International Research Journal on Engineering*, **1**(2): 49-56.

Vanorio, T., Prasad, M., and Nur, A. (2003), Elastic properties of dry clay mineral aggregates, suspensions and sandstones, *Geophysical Journal International*, **155**(1): 319-326.

Wanyonyi, S. O. (2004), An Engineering Geological characterization of Tropical Clays. Case study: Clay soils of Nairobi, Kenya, MSc. Thesis, pp 42-65.

Weitkamp, T., Diaz, A., David, C., Pfeiffer, F., Stampanoni, M., Cloetens, P and Ziegler, E. (2005), X-ray phase imaging with a grating interferometer, *Optics Express*, **13**(16): 6296-6304.

APPENDICES

APPENDIX 1: Atterberg readings for black soil

Container No	1	2	3	4	PL	PL
Cone penetration (mm)	15.9	18.0	20.3	22.1	-	-
Mass of tin+ wet soil (m_2) g	74.1	72.9	58.4	67.2	35.0	36.5
Mass of tin+ dry soil (m_3) g	60.8	59.2	49.2	55.6	33.6	35.2
Mass of tin (m_1) g	31.4	29.6	29.8	31.6	28.8	30.6
Mass of water ($m_4= m_2- m_3$) g	13.3	13.7	9.2	11.6	1.4	1.3
Mass of dry soil ($m_5= m_3- m_1$) g	29.4	29.6	19.4	24.0	48.0	46.0
%Moisture Content (m_4/ m_5)x100=w	45.2	46.3	47.4	48.5	29.2	28.3
Average Moisture content (w)%	45.2	46.3	47.4	48.5	28.8	

APPENDIX 2: Atterberg limits for Ilesi brown soil

Container No	1	2	3	4	5	PL	PL
Cone penetration (mm)	16.0	17.8	18.1	20.1	22.0	-	-
Mass of tin+ wet soil (m_2) g	79.6	73.1	68.4	79.4	78.8	35.8	38.6
Mass of tin+ dry soil (m_3) g	69.2	61.6	58.0	65.6	65.4	34.8	37.4
Mass of tin (m_1) g	32.2	29.8	29.6	28.8	30.6	30.8	31.4
Mass of water($m_4= m_2- m_3$) g	12.4	11.5	10.4	13.8	13.4	1.0	1.2
Mass of dry soil ($m_5= m_3- m_1$)	35.0	31.8	28.4	36.8	34.8	4.8	6.0
Moisture Content(m_4/ m_5)x100=w%	35.4	36.2	36.6	37.5	38.5	20.1	20.0
Average Moisture content (w)%	35.4	36.2	36.6	37.5	38.5	20.0	

APPENDIX 3: Atterberg limits data for Ilesi grey soil

Container No	1	2	3	4	PL
Cone penetration (mm)	15.8	18.2	20.1	21.8	-
Mass of tin+ wet soil (m_2) g	68.2	79.5	68.8	65.5	39.2
Mass of tin+ dry soil (m_3) g	59.6	68.2	59.0	57.8	38.2
Mass of tin (m_1) g	31.0	31.2	27.4	33.6	33.4
Mass of water($m_4= m_2- m_3$) g	8.6	11.3	9.8	7.6	1.0
Mass of dry soil ($m_5= m_3- m_1$)	28.6	37.0	31.6	24.2	48.0
Moisture Content(m_4/ m_5)x100=w%	30.1	30.5	31.0	31.4	20.8
Average Moisture content (w)%	30.1	30.5	31.0	31.4	21.5

APPENDIX 4: Sieve analysis for black clay

On Sieve (mm)	A sieve, g	B sieve+ soil ,g	C=B-A Retained ,g	D %retained	E=∑ D Cumulative % retained	F=100-E % Finer
2.000	405.7	406.9	1.2	0.5	0.5	100
1.000	344.9	346.3	1.4	0.6	1.1	99
0.600	403.9	410.0	6.1	2.5	3.6	96
0.425	294.8	303.5	8.7	3.6	7.2	93
0.300	287.0	297.3	10.3	4.3	11.5	89
0.212	346.3	355.4	9.1	3.8	15.3	85
0.150	290.3	299.8	9.5	3.9	19.2	81

APPENDIX 5: Hydrometer tests for black clay

Time	Time elapsed(min)	Rh^1	Rh= Rh^1 +C_m	D(mm)	Rh+ mt-x	K%	% Finner K.K_1/100
11.55	0.5	18.0	18.4	0.095	14.4	64.5	75
11.56	1	17.5	17.9	0.07	13.9	62.2	70
11.57	2	15.5	15.9	0.052	11.9	55.9	67
11.59	4	14.5	14.9	0.036	10.9	52.2	65
12.07	8	12.5	12.9	0.025	8.9	47.8	63
12.10	15	12.0	12.4	0.018	8.4	45.5	55
12.25	30	11.0	11.4	0.0098	7.4	42.8	47
12.55	60	10.0	10.4	0.0094	6.4	41.1	44
1.55	120	9.0	9.4	0.0065	5.4	39.5	40
3.55	240	7.5	7.9	0.0045	5.3	37.5	38
11.55	1440	5.0	5.4	0.0021	4.4	37.7	38

APPENDIX 6: Sieve analysis for the brown clay

On Sieve (mm)	A sieve, g	B Sieve + soil, g	C=B-A Retained ,g	D %retained	E=∑ D Cumulative % retained	F=100-E % Finer
2.000	405.7	423.1	17.4	7.1	7.1	100
1.000	344.9	361.4	16.5	6.7	13.8	86
0.600	403.9	433.2	29.3	12	25.8	74
0.425	294.8	312.2	17.4	7.11	32.9	67
0.300	287.0	302.2	15.2	6.2	39.1	61
0.212	346.3	357.7	11.4	4.7	43.8	56
0.150	290.3	301.4	11.1	4.5	48.3	52

APPENDIX 7: Hydrometer tests for brown soil

me	Time elapsed(min)	Rh^1	Rh= Rh^1 +C_m	D(mm)	Rh+mt-x	K%	%Finner K.K_1/100
12.00	0.5	18	18.4	0.095	14.4	45.5	46
12.01	1	16	16.4	0.068	12.4	45.1	45
12.02	2	15	15.4	0.049	11.4	40.5	41
12.04	4	14	14.4	0.032	10.4	37.8	38
12.08	8	13.5	13.9	0.026	9.9	36.5	37
12.15	15	13	13.4	0.016	9.4	34.2	34
12.30	30	12.5	12.9	0.0096	8.9	31.8	32
1.00	60	11.5	11.9	0.0094	7.9	30.1	30
2.00	120	10.5	10.9	0.007	6.9	28.5	29
4.00	240	10	10.4	0.005	6.4	27.1	27
12.00	1440	9	9.4	0.0018	5.4	25.5	26

APPENDIX 8: Sieve analysis for grey clay

On Sieve (mm)	A sieve, g	B sieve+ soil, g	C=B-A retained, g	D %retained	E=$\sum D$ Cumulative % retained	F=100-E % Finer
2.000	405.7	410.4	4.7	1.9	1.9	100
1.000	344.9	351.2	6.3	2.6	4.5	96
0.600	403.9	421.4	17.5	7.2	11.7	88
0.425	294.8	309.9	15.1	6.2	17.9	82
0.300	287.0	304.9	7.9	7.3	25.2	75
0.212	346.3	365.7	19.4	8.0	33.2	67
0.150	290.3	313.7	23.4	9.6	42.8	65

APPENDIX 9: Hydrometer tests for grey clay

Time	Time elapsed(min)	Rh^1	Rh= Rh^1 +C_m	D(mm)	Rh+mt-x	K%	%Finner K.K_1/100
11.50	0.4	17	17.4	0.096	13.4	56.5	57
11.51	1	15	15.4	0.072	11.4	51	51
11.52	2	13.5	13.9	0.05	9.4	48.6	50
11.54	4	12.5	12.9	0.034	8.9	48.2	49
11.58	8	12.5	12.9	0.025	8.9	44.8	49
12.05	15	11.5	11.9	0.018	7.9	41.3	41
12.2	30	11	10.4	0.008	7.4	40.1	40
12.5	60	10	10.4	0.0095	6.4	36.4	36
1.5	120	10	9.4	0.0068	6.4	36.4	36
3.5	240	9	8.4	0.0045	5.4	34.7	35
11.5	1440	8	8.3	0.002	4.4	32.3	32

APPENDIX 10: Percentage elemental composition of Butali grog in oxide form

Elements	% Butali±SE
SiO_2	58.651±0.654
Al_2O_3	19.144±0.908
Fe_2O_3	10.701±0.045
K_2O	2.880±0.03
CaO	6.031±0.036
TiO_2	1.400±0.038
SO_3	0.624±0.045
SrO	0.110±0.002
Rb_2O	0.066±0.002
V_2O_5	0.060±0.019
CuO	0.147±0.005
MnO	0.185±0.01

APPENDIX 11: Proposed tempers

Elements	% Butali SCBA-F±SE	% Butali SCBA-P±SE
SiO_2	78.532±0.563	63.723±0.611
Fe_2O_3	2.888±0.017	4.390±0.023
K_2O	10.147±0.047	16.391±0.068
CaO	4.807±0.033	9.204±0.054
TiO_2	0.309±0.016	0.376±0.020
SO_3	1.205±0.045	2.206±0.062
SrO	0.041±0.001	0.027±0.001
Rb_2O	0.023±0.001	0.00
ZrO_2	0.018±0.001	0.00
P_2O_5	1.414±0.080	2.821±0.117
CuO	0.040±0.002	0.00
MnO	0.540±0.009	0.791±0.012
ZnO	0.035±0.002	0.07±0.003

APPENDIX 12: EDX Spectrum for black clay

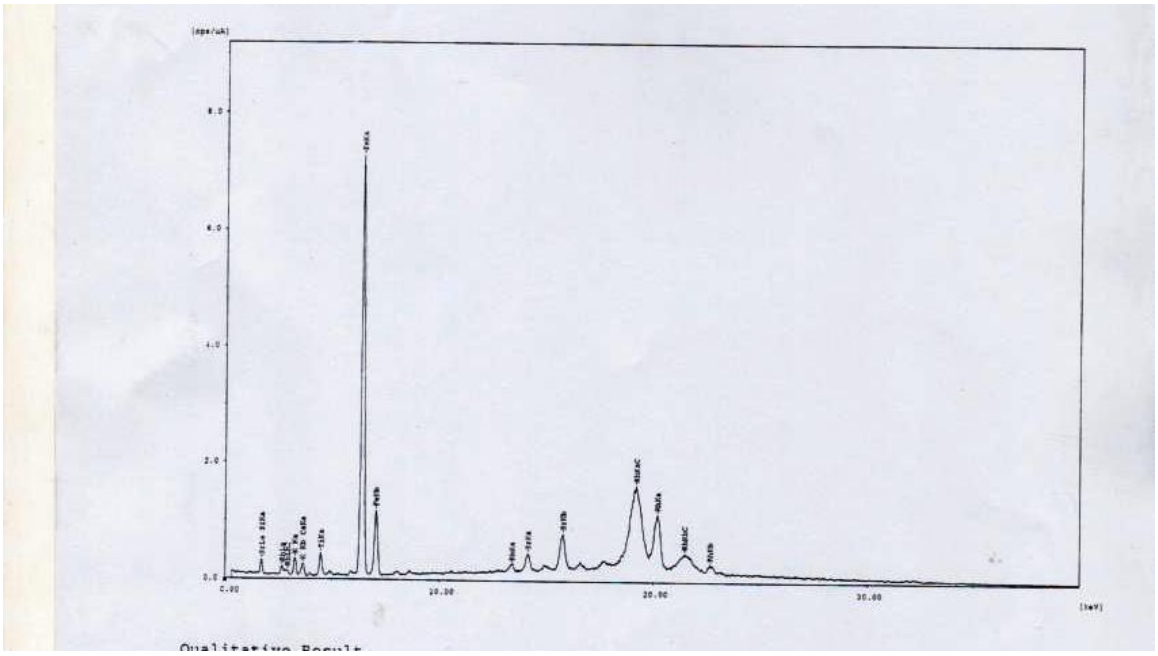

APPENDIX 13: EDX Spectrum for brown clay

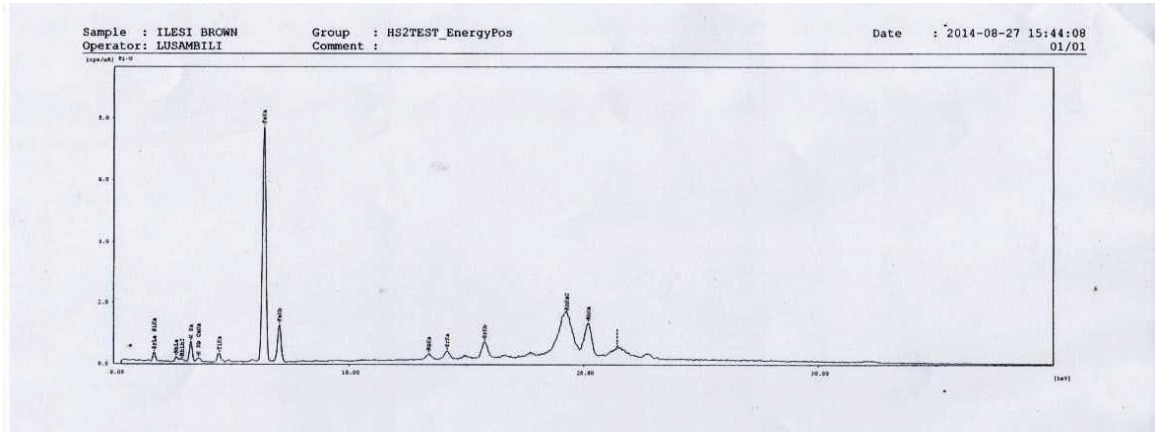

APPENDIX 14: EDX Spectrum for grey clay

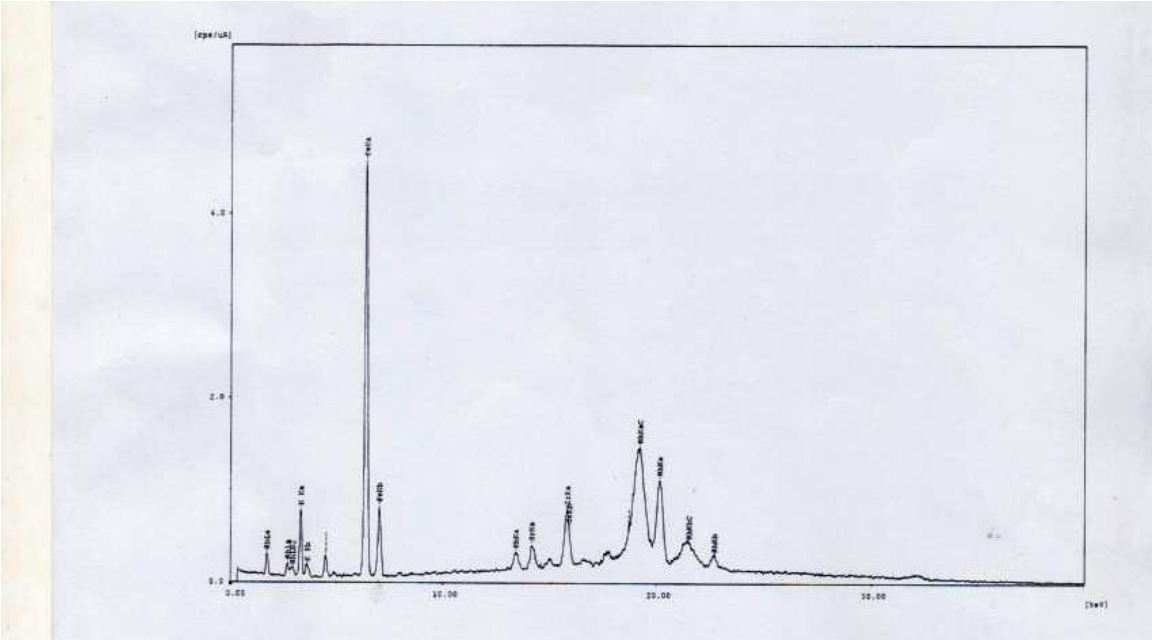

APPENDIX 15: EDX Spectrum for Ilesi grog

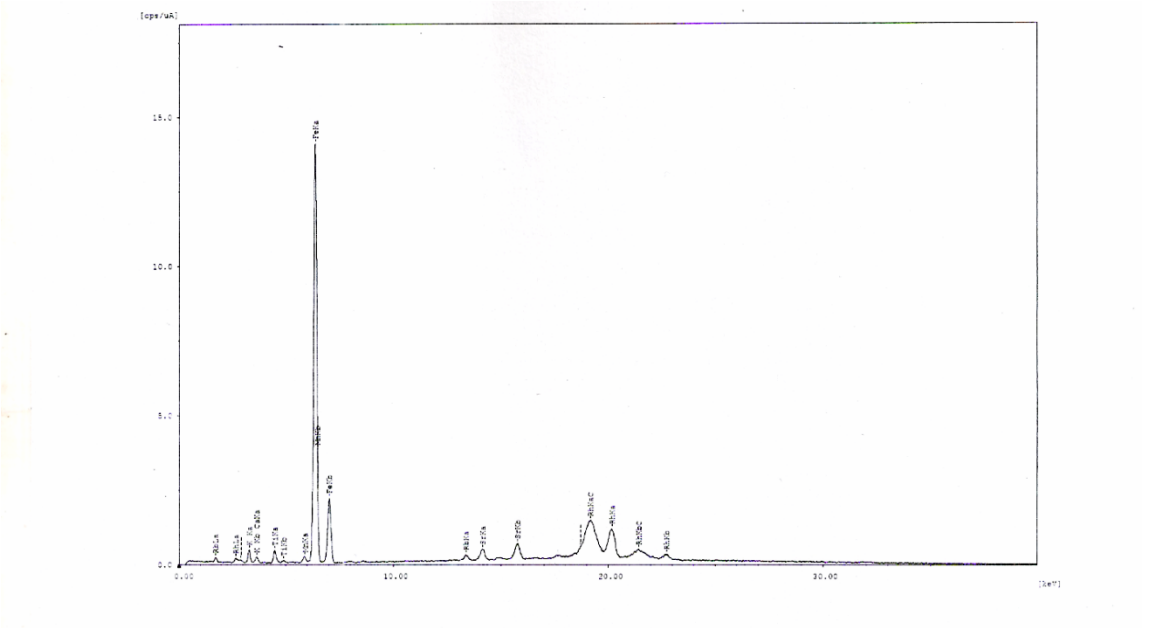

APPENDIX 16: EDX Spectrum of Butali grog

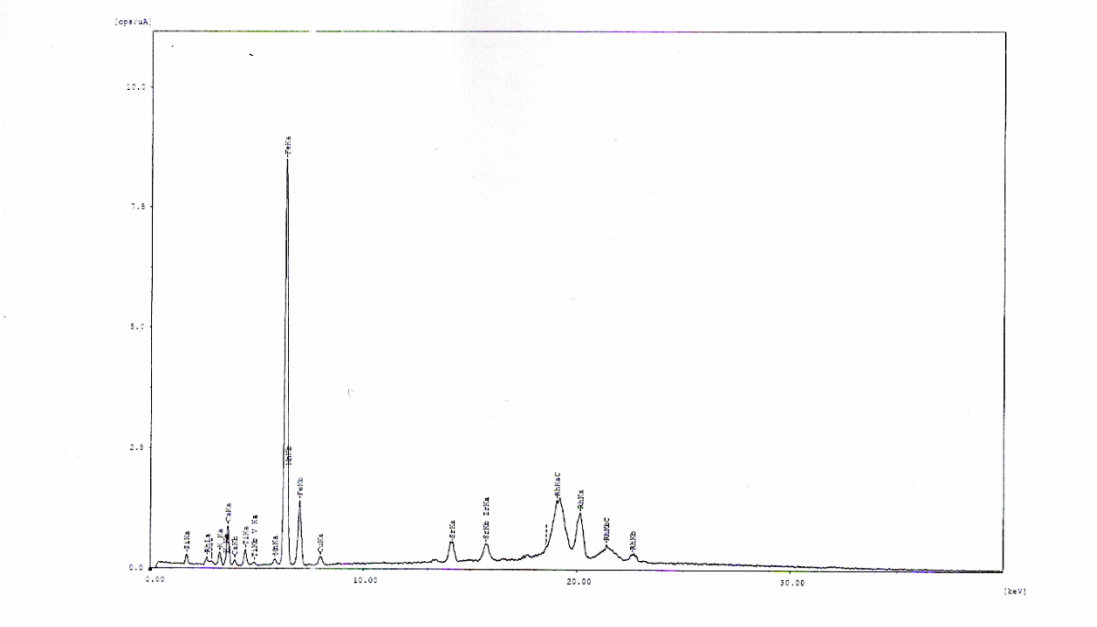

APPENDIX 17: EDX spectrum for Butali SCBA